

Duquesne University

Duquesne Scholarship Collection

Electronic Theses and Dissertations

Summer 2006

Solid-Phase Induction of *Xenopus Laevis* Animal Caps by FGF-2: A Novel Developmental Approach

Peter Maropis

Follow this and additional works at: <https://dsc.duq.edu/etd>

Recommended Citation

Maropis, P. (2006). Solid-Phase Induction of *Xenopus Laevis* Animal Caps by FGF-2: A Novel Developmental Approach (Master's thesis, Duquesne University). Retrieved from <https://dsc.duq.edu/etd/875>

This Immediate Access is brought to you for free and open access by Duquesne Scholarship Collection. It has been accepted for inclusion in Electronic Theses and Dissertations by an authorized administrator of Duquesne Scholarship Collection.

**Solid-Phase Induction of *Xenopus Laevis* Animal Caps by FGF-2: A
Novel Developmental Approach**

A Thesis
Presented to the Bayer School of Natural and Environmental Sciences
Department of Biological Sciences
Duquesne University

In partial fulfillment of the requirements
for the degree of Masters of Science

by

Peter S. Maropis

Thesis Advisor: John S. Doctor, Ph.D.

**Thesis Committee:
Phil Campbell, Ph.D.
Richard P. Elinson, Ph.D.
Jana Patton-Vogt, Ph.D.**

Name: Peter Stewart Maropis

Thesis Title: Solid-Phase Induction of *Xenopus Laevis* Animal Caps
by FGF-2: A Novel Developmental Approach

Degree: Masters of Science

Date: 15 May 2006

Approved: _____
Dr. Richard P. Elinson, Committee Member
Department of Biological Sciences, Duquesne University

Approved: _____
Dr. Phil G. Campbell, Committee Member
Institute for Complex Engineered Systems, Carnegie Mellon University

Approved: _____
Dr. Jana Patton-Vogt, Committee Member
Department of Biological Sciences, Duquesne University

Approved: _____
Dr. Joseph R. McCormick, Interim Department Chair
Department of Biological Sciences, Duquesne University

Approved: _____
Dr. David W. Seybert, Dean
Bayer School of Natural and Environmental Sciences, Duquesne University

Abstract

Cells become different in development due to induction, a ligand-mediated cell interaction. This type of interaction is an area of intense research for developmental biologists studying the effects of different growth factors (during development). The conventional approach to induction with *Xenopus Laevis*, African Clawed Frog, employs placing cells or tissues in a growth factor solution. This design reveals an enormous amount of information and insight into developmental processes, but it is not an accurate approach to simulate *in vivo* conditions. Here, I use a novel approach, termed solid-phase induction, as a more realistic and controllable approach. I utilize a glass surface coated with fibrin to act as a surface to adhere growth factors for Solid-phase presentation. This method will not only provide a more accurate representation of cell-cell inductions, but will also add an increased level of control in presenting growth factors. This approach will be used to answer developmental questions that involve spatially oriented induction and differential induction by different concentration gradients or specific patterns of a number of growth factors.

Acknowledgments

I would like to thank everyone who has helped and supported me through the past two years at Duquesne University. Without the help of everyone, I would not have been able to conduct this exciting research: Dr. Richard Elinson, for the countless questions and discussions about my research as well as the world of baseball and the Steelers; Dr. Phil Campbell, for the motivation and drive to continue through all of the obstacles encountered, as well as my funding to do my experiments and making my life easier by purchasing the Gastromaster; past and present members of the Doctor lab; past and present members of the Elinson lab; members of the Campbell lab, especially Eric Miller for providing my fibrin slides and answering my endless technical questions; Pam and Judy for all their help in the Biology office and a means to brighten every one of my days at Duquesne University.

Finally, but certainly not least I would like to thank Dr. John Doctor for changing the way I viewed science and education in general. Without the superior mentoring and support from Dr. Doctor I would not be where I am today. He was the motivation that drove me to want to be the best researcher, student, and person that I could be. He taught me not to accept average but to pursue perfection. I am truly grateful for everything that he did for me. He will never be far from my thoughts.

Table of Contents

Title page.....	1
Signature Page.....	2
Abstract.....	3
Acknowledgments.....	4
Table of contents.....	5
List of Figures.....	7
Introduction.....	8
Signal Transduction	8
<i>Xenopus</i> Early Development.....	11
<i>Xenopus</i> Tissue Induction.....	13
Mesoderm Induction.....	16
FGF as a Mesoderm Signaling Molecule.....	17
Definition of solid-phase.....	18
Rationale for engineering solid-phase spatial patterns of hormones on fibrin and fibronectin matrices.....	20
Plan of Thesis.....	22
Rationale	
Experimental Approach	
Material and Methods.....	23
<i>Xenopus</i> Embryos.....	23
Animal Cap Isolation.....	24
Liquid-phase induction.....	24
Design of the solid-phase chamber.....	25
Fibrin Slide Preparation.....	25
Solid-phase Induction.....	26
RNA extraction.....	27
RT-qPCR.....	28
1 step RT-qPCR Amplification.....	28
Separation and Analysis of Data.....	29
<i>In situ</i> Hybridization of Animal Caps.....	30
Fixing Animal Caps for <i>in situ</i>	30

<i>Xbra</i> Plasmid Midi Prep	30
Restriction Digest of <i>Xbra</i> Plasmid	31
Transcription of the sense and antisense probes	32
<i>In situ</i> hybridization	33
Photography of animal caps	36
Results	37
Liquid-phase FGF-2 induction	37
Solid-phase Chamber Design	37
Establishing an RT-qPCR Assay for transcription detection	38
RT-qPCR Detection of <i>Xbra</i> in liquid-phase and solid-phase FGF-2 Induction	39
<i>In situ</i> hybridization of animal caps induced with FGF-2	40
Figures	42
Discussion	59
Liquid-phase induction with FGF-2	59
Solid-phase chamber design	59
Solid-phase induction with FGF-2	60
RT-qPCR of solid-phase FGF-2 induced animal caps	60
<i>In situ</i> of animal caps induced with solid-phase FGF-2	61
New solid-phase chamber design	62
Future experiments with solid-phase growth factor presentation	63
Conclusion	65
References	66

List of Figures

Fig. 1: Germ Layer Orientation	11
Fig. 2: Gastrulation of <i>Xenopus</i> Embryo	12
Fig. 3: Animal cap isolation	42
Fig. 4: Expression of the mesoderm marker <i>Xbra</i> in response to FGF-2 in liquid-phase	44
Fig. 5: Inhibition of animal cap healing	46
Fig. 6: Solid-phase chamber design	48
Fig. 7: <i>Xbra</i> expression in response to FGF-2, presented in liquid-phase or solid-phase	50
Fig. 8: <i>In situ</i> of animal caps exposed to FGF-2	52
Fig. 9: New solid-phase chamber design	55
Fig. 10: Model for neural induction experiment	57

Introduction

I. Signal Transduction:

Signal transduction refers to the passage of a signal from the outside of the cell to the inside of the cell. There are many different types of signal transduction events, and can be as simple as a ligand binding to its receptor allowing the passage of molecules through a membrane channel. Some signal transduction events can be very complex, for example where the ligand-receptor complex initiates the phosphorylation of a number of proteins inside the cell.

During embryonic development, many signals are used in patterning, migration and differentiation. These signals must have a specific means to act on their intended cells. Signal transduction is one way in which this is possible. Cells must contain all the elements of the signal transduction cascade to be able to elicit the specific response intended by the ligand.

There are five main signal transduction pathways that are utilized during development: 1) the receptor tyrosine kinase (RTK) pathway, 2) the Smad pathway, 3) the JAK-STAT pathway, 4) the Wnt pathway, and 5) the Hedgehog pathway (Gilbert, 2000). The RTK pathway is activated by binding of a specific ligand or a small class of ligands per receptor. Some of these ligands are members of the Fibroblast Growth Factor (FGF) family (Dailey et al., 2005), the Endothelial Growth Factor (EGF) family, and the Platelet Derived Growth Factor (pDGF) family. Binding of the ligand causes the receptors to form a homodimer which activates the intracellular domain by autophosphorylation. Once phosphorylated an adaptor protein binds and then activates

a powerful intracellular transducer, a G-protein. The rest of the cascade of events depends on the cell being signaled and the ligand that was delivered (Gilbert, 2000). Some of the developmental processes driven by this signaling cascade include proliferation, growth arrest, differentiation or apoptosis (Dailey et al., 2005).

The next class is the Smad pathway. Activation is initiated by binding of a member of the transforming growth factor- β (TGF- β) family to a type II TGF- β receptor, which forms a heterodimer with a type I receptor (Gilbert, 2000). Once again, autophosphorylation takes place but on a serine or threonine residue. After activation, the type I receptor activates the Smad proteins by phosphorylation (Shi and Massague, 2003). Members of the bone morphogenic protein (BMP) family activate the Smad 1 and 5 proteins, while activin and other members of the TGF- β family activate the Smad 2 and 3 proteins. In both cases, these Smad proteins will form a transcription factor complex with Smad 4 to enter the nucleus (Gilbert, 2000).

The JAK-STAT signal transduction pathway is named after its transcription factors, the signal transducers and activators of transcription, or STATs. They are commonly activated by being phosphorylated from the FGF receptors and the JAK family of tyrosine kinases after binding by a variety of cytokines, hormones and growth factors (Valentino and Pierre, 2006). This signal transduction pathway is very important in the differentiation of blood cells, regulation of fetal bone growth, and others (Gilbert, 2000).

The proteins of the Wnt family are paracrine factors that bind and activate the transmembrane receptors of the Frizzled family (Gilbert, 2000). The Frizzled proteins frequently activate the protein Disheveled which inhibits glycogen synthase kinase-3.

This is only one possible pathway, but there are many different roads that this transduction pathway can take depending on the proteins present in the cell. The Wnt pathway is commonly activated to turn on specific Wnt activated genes during development, to control actin and microtubular growth, as well as to release of Ca^+ from the endoplasmic reticulum (Gilbert, 2000). The regulation of Wnt signaling has also been implicated in the important early developmental process that initiates cardiac development (Eisenberg and Eisenberg, 2006).

The final signal transduction pathway is the Hedgehog pathway. The proteins of the hedgehog family are of fundamental importance during development as well as maintaining tissue patterns in adult organisms (Bijlsma et al., 2004). These proteins are paracrine factors that bind to the membrane receptor Patched (Ptc.) (Bijlsma et al., 2004). However, Ptc. is not a signal transducer itself, but rather it is attached to one, Smoothed (Smo.). When bound to Ptc, Smo is inactive. The inhibition of Smo subjects a zinc finger transcription factor to remain tightly contained in a microtubule-bound protein complex. While in this complex the N-terminal region of the transcription factor will be subject to cleavage. This cleaved portion of the transcription factor acts as a repressor and enters the nucleus to inhibit transcription of hedgehog specific genes (Bijlsma et al., 2004). Once a hedgehog member is bound to Ptc the Smo protein is released. This will in turn allow for the removal of the zinc finger transcription factor from the microtubule-bound complex leading to hedgehog specific gene transcription (Bijlsma et al., 2004). This pathway is involved in many developmental processes but is imperative during vertebrate limb and neural differentiation (Gilbert, 2000).

II. *Xenopus* Early Development:

Development of *Xenopus laevis*, the African clawed frog, begins with early patterning and formation of the embryo. This process is very intricate with multiple signals working together to direct differentiation as well as shaping and migration of the tissues into their proper orientation. This initial harmonious organization by multiple signaling events leads to the development of specialized organs and body structures that work together as the blueprint of the adult organism.

In the early developing embryo, the first example of this precise molecular signaling is the specification of the embryonic germ layers. The establishment of these germ layers entails the following: cellular asymmetries, inductive interactions, maternal factors, and mechanical movements (Shook et al., 2004). Each germ layer arises as disparate cell populations, within the embryo, with ectoderm at the top of the embryo, endoderm at the bottom of the embryo, and mesoderm between the two (Fig.1) (Shook et al., 2004). The allocation of each germ layer is so precise that the proportion of each is consistent from individual to individual (Wardle and Smith, 2004).

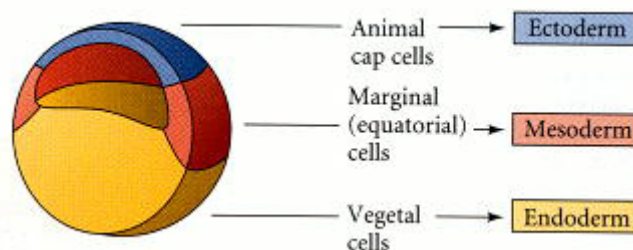


Fig. 1 Germ Layer Orientation.

Initial orientation of the three germ layers at the blastula stage of *Xenopus* development (Fig. 10.21A from Gilbert, 2000 by permission from Sinauer Inc).

Once the three germ layers are set up, the embryo undergoes the process of gastrulation (Fig. 2). During gastrulation the three germ layers migrate to their final positions with the ectoderm lining the outer surface of the embryo and the mesoderm and endoderm to the inside of the embryo (Maurus and Kuhl, 2004). This rearrangement initiates most of the inductive events of the embryo that will lead to the formation of the adult organism. It also leads to the transformation of a spherical embryo to one that is elongated along the anterior-posterior axis (Maurus and Kuhl, 2004).

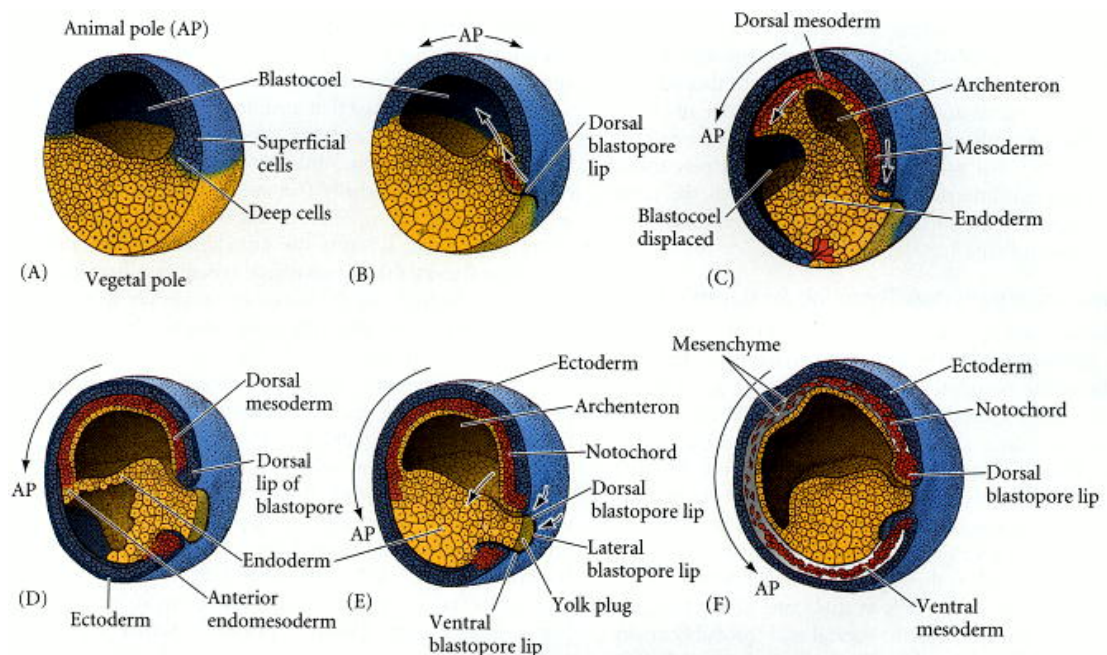


Fig. 2 Gastrulation of *Xenopus* Embryo.

Detailed depiction of the movements that take place during *Xenopus* gastrulation. The diagram begins with an embryo in the blastula stage where the three germ layers are already set up. The process of gastrulation is the initial migration and differentiation of the cells of the embryo to set up the future body plan of the embryo from the initial three germ layers.

(Fig. 10.7 from Gilbert, 2000 by permission from Sinauer Inc)

III. *Xenopus* tissue induction:

The actual process of induction was well described by Pander in 1817, “each germ layer is not yet independent enough to indicate what it truly is; it still needs the help of its sister travelers, and therefore, although already designated for different ends, all three influence each other collectively until each has reached an appropriate level.” Today, this process being described by Pander can be termed induction.

During *Xenopus* development, there are many examples of induction. Some of the most well known examples include neural induction, midbrain-hindbrain induction, dorsal and ventral fin induction, limb organogenesis and mesoderm induction.

Once the three germ layers have been set up in the early *Xenopus* embryo the process of gastrulation takes place where cells from the surface invaginate through the blastopore and migrate underneath the ectoderm. In 1924, Hilde Mangold, a student of Hans Spemann, established the concept that neural induction took place with the interactions of the dorsal lip of the blastopore and the overlying ectoderm during gastrulation (Stern, 2005). This dorsal lip would later be called the Spemann organizer. In the 1990's, three genes coding for proteins that had neuralizing activity were found to emanate from the organizer, Noggin, Follistatin, and Chordin (Smith et al., 1993), (Hemmati-Brivanlou et al., 1994), (Sasai et al., 1995). These molecules were BMP binding proteins, and once bound would block the action of BMP with the BMP receptor (Piccolo et al., 1996). These findings led to the default mode of neural induction where the inherent ability of the ectoderm to differentiate into neural tissue is inhibited by BMP (Hemmati-Brivanlou and Melton, 1997). This has been the current understanding of neural induction since then, but recent evidence indicates that other

molecules such as the FGFs, are also necessary for neural induction (Stern, 2005). It is clear that there are multiple different signaling molecules and transcription factors that must be coordinated not only in a spatial arrangement but also in a concentration dependent manner for neural induction to take place.

Once neural induction has commenced, this neural tissue must be further differentiated into the multiple neural fates. Tissue that has been induced to differentiate to a neural fate in response to noggin or chordin shows only anterior specification leading to the idea that these factors alone are not sufficient to pattern the newly formed neural tissue (Song et al., 1999). Although little is known about the specifics of neural patterning, there are two candidates, xGCNF, a nuclear orphan receptor is a good candidate for neural patterning, and retinoic acid (RA) (Song et al., 1999; van der Wees et al., 1998). xGCNF shows an expression pattern and activity that can be reliably linked to the patterning of the midbrain-hindbrain region (Song et al., 1999). The second candidate, RA, has been shown to have a dramatic affect on hindbrain formation. If there is too much RA present or the retinoic acid receptors are over expressed there is a dramatic increase in the volume of the hindbrain (van der Wees et al., 1998).

In *Xenopus*, development of a dorsal/ventral fin provides the means for tadpole locomotion, prior to the formation of the limbs. This fin begins to develop at the tail bud stage along the trunk and tail of the embryo (Tucker and Slack, 2004). Both the dorsal and ventral portions of the fin consist of mesenchyme derived from neural crest cells. Not only do these neural crest cells provide the mesenchyme that make up the fin, but they are also responsible for the induction of the epidermis of the fin (Tucker

and Slack, 2004). This induction is restricted to the dorsal half of the fin whereas the ventral half is receiving its induction via a different source (Tucker and Slack, 2004). Although the specific molecules involved in this inductive process are unknown at present, this is another example of a single tissue being induced differentially by distinct sources of molecules interacting with in an individual tissue.

The inductive process of limb initiation and outgrowth in other organisms has been centered on the interactions of two FGF molecules in these tissues. FGF-10 is expressed in the mesenchyme which induces the expression and maintenance of FGF-8 in the surrounding limb bud ectoderm. In turn, FGF-8 also feeds back to maintain the expression of FGF-10 in the mesenchyme to allow for limb outgrowth (Martin, 1998).

Limb development has been an understudied area in *Xenopus* because of the late onset during development. Recently however, this topic has received more attention because of the implications of limb regeneration. *Xenopus* has an ability to regenerate its limbs during a period of its development. The developing limb is primarily composed of mesenchymal tissues derived from the lateral plate mesoderm with a surrounding layer of ectoderm. It has been shown that FGF-10 soaked beads, introduced to this mesenchyme, will initiate limb formation (Yokoyama et al., 2001). It is hypothesized that limb development in the *Xenopus* is driven by the interactions of FGF molecules as well. Once again, here is an inductive process that integrates more than one signaling molecule to allow, in this case, the development of the limb.

IV. Mesoderm Induction:

One of the most well studied induction events is that of mesoderm tissue. To set up the initial three germ layers (ectoderm, mesoderm, and endoderm (Fig. 2)) the mesoderm in the early embryo must be induced. Mesoderm induction happens right before gastrulation in the *Xenopus* embryo, and represents the first cell-cell interaction (Eimon and Harland, 2002). The induction of this tissue stems from the interactions between the ectoderm and the endoderm. This interaction was shown through recombinant experiments performed by Slack (1991) where blastula embryos were dissected and sandwiches were made with vegetal pole explants (prospective endoderm) and animal caps (prospective ectoderm). Slack concluded that the ectoderm was induced to form mesoderm through endodermal signaling.

Through the years, there have been many candidate ligands for this induction such as bFGF, Activin, Derriere, and *Xenopus* nodal related (Slack, 1991; Smith et al., 1995; Sun et al., 1999; Thomsen and Melton, 1993). More recent research has led to the discovery that there is a maternally encoded transcript that must be present to generate the production of this mesoderm-inducing signal. This maternal transcription factor, VegT, is localized in the vegetal cortex of the oocyte. When inhibited in oligonucleotide depletion experiments, there was an inhibition of mesoderm signaling and formation (Zhang et al., 1998). Kofron et al. (1999) hypothesized that VegT must be responsible for promoting the expression of the natural in vivo mesoderm inducer. Indeed VegT directly regulates the expression of Derriere and Xnr4 in the *Xenopus* embryo (Kofron et al., 1999; Yasuo and Lemaire, 1999). Both the Xnrs and Derriere act as molecular morphogens, eliciting a full range of mesoderm inductions in a dose

dependent manner (Schier and Shen, 2000). Even though bFGF and Activin may play roles in mesoderm formation, there has been a shift in thinking towards the Xnrs and Derriere as the natural mesoderm inducers. This new idea is based on the results that they both act as gradient dependent mesoderm inducers and most importantly, that their expressions are regulated by the maternally encoded VegT RNA.

V. FGF as a mesoderm signaling molecule:

In 1987, Slack and colleagues discovered the first mesoderm inducer, basic FGF (Slack et al., 1987). Once word spread of the first mesoderm inducer being bFGF, the scientific community considered this to be a good candidate as the endogenous mesoderm-inducing signal in *Xenopus* (Isaacs et al., 1994). This was not a blind idea because it had an evolutionary background. bFGF signaling is required for mesoderm induction in the vertebrates, mouse and zebrafish, as well as the primitive chordate *Ciona* (Nishida, 2002).

The FGFs constitute a family of peptide growth factors that after binding to their tyrosine kinase receptors, induce receptor dimerization and autophosphorylation of intracellular tyrosine residues (Mohammadi et al., 1996). One of the consequences of receptor autophosphorylation is to activate the GTPase Ras, setting off a cascade of kinases including Raf, MEK, and finally MAPK which ultimately results in processes such as the induction of gene expression required in mesoderm induction in *Xenopus* (Fambrough et al., 1999).

bFGF expression is only seen in a small region between the ectoderm and endoderm (Smith, 1989). bFGF was ruled out as the primary, vegetal-localized

mesoderm inducer because they were only localized to the early mesoderm ring, and then later around the blastopore.

Further research has led biologists to believe that bFGFs role in mesoderm formation is that of a competence factor (Bottcher and Niehrs, 2005). bFGF must be present in the prospective mesoderm to allow for the full range of mesoderm induction via the primary mesoderm inducers. This has been demonstrated by knocking out the bFGF receptor as well as over expressing the receptor. When activin or the Xnrs were introduced to animal caps that had altered bFGF receptors, mesoderm induction was interrupted (Cornell and Kimelman, 1994). Once the Xnrs act on the presumptive mesoderm tissue, a T-box transcription factor, Xbra is expressed (Cornell and Kimelman, 1994; Loose and Patient, 2004). It is now believed that this expression of Xbra is responsible for the expression of FGF in the presumptive mesoderm of the marginal zone. Once FGF expression is present, it maintains the expression of Xbra (Schulte-Merker and Smith, 1995). This feedback loop is necessary for proper mesoderm induction.

VI. Definition of solid-phase:

To date, most of these developmentally important signaling molecules have been assayed using *Xenopus* animal caps and liquid-phase growth factors. The *Xenopus* embryo is allowed to develop to stage 9 (Nieuwkoop, 1956), and then the ectoderm (animal cap) is removed (Fig. 3). This tissue is capable of being induced into multiple tissue lineages depending on the growth factor presented. Once the caps have been isolated they are cultured in a liquid-phase growth factor solution and then assayed for

tissue specific gene expression. The term “liquid-phase” refers to soluble, freely diffusible signaling molecules. In contrast, the term “solid-phase” refers to the immobilization of a signaling molecule to a matrix (Campbell and Andress, 1997; Campbell and Andress, 1997; Campbell et al., 1999; Campbell et al., 1994; Durham et al., 1999; Fan et al., 2000; Sakiyama-Elbert and Hubbell, 2000; Sakiyama-Elbert and Hubbell, 2000). There are multiple ways to immobilize a signaling molecule to a matrix, but they can be grouped into two broad categories: (1) adsorption via non-specific protein-protein interactions (2) highly specific adsorption with high affinity interactions, such as heparin binding domains. The ability of these signaling molecules to remain bound to the matrix depends on the binding affinity, number of binding sites, and the presence of competitive binding molecules. Two of the methods to being utilized to immobilize the signaling molecules are: (1) by directly pipetting the desired growth factor to the fibrin coated glass slide and allowing it to dry, or (2) printed patterns deposited with a custom inkjet system that was developed for precise printing applications. This inkjet is a MicroJet™ piezoelectric drop-on-demand device with a 30um diameter nozzle (MicroFab Technologies, Inc., Plano, TX) (Campbell et al., 2005).

The bioavailability of FGF-2 and response of human MG-63 cells to the printed pattern have previously been demonstrated (Campbell et al., 2005). The presence of printed FGF-2 does not alter its attachment to human MG-63 cells prior to their response to the growth factor (Campbell et al., 2005). These cells proliferate, the expected response to FGF-2, when seeded on the solid-phase printed FGF-2 (Miller et al., 2006).

VII. Rationale for engineering solid-phase spatial patterns of hormones on fibrin and fibronectin matrices:

Solid-phase presentation of signaling molecules, rather than liquid-phase, is of biological relevance, since endogenous solid-phase extracellular hormone gradients are present in an array of developmental models (Gurdon and Bourillot, 2001; Ruhrberg et al., 2002, Strigini and Cohen, 2000). This solid-phase approach is plausible because many signaling molecules bind to extra cellular matrices (ECM), either directly or through intermediate binding proteins (Rifkin et al., 1999). Persistent patterns can be set up by sequestering signaling molecules in the ECM to control their spatial arrangement. An example is proteoglycans, a class of ECM and cell surface molecules capable of binding and sequestering hormones in an arranged spatial pattern (Bernfield et al., 1999). Signaling molecules contain heparin binding domains within their structure that are capable of forming these extracellular signaling patterns (Ohkawara et al., 2002).

ECMs, in particular fibronectin (FN), are able to sequester signaling molecules to allow for gradient patterned presentations. They are also responsible for the movement and guidance of cells during differentiation. During *Xenopus* gastrulation, the basic body plan of the embryo is set up by the movement of the involuting cells from the dorsal lip along a pre-existing ECM (Ramos and DeSimone, 1996). This movement, conducted over FN, allows for the spatial orientation of the different cell types. It also allows for proper placement of cells that are capable of inducing differential tissue induction by releasing signaling molecules to the overlying cell layers. An example of this is the movement of the dorso-mesodermal tissues ventrally underneath the

ectoderm, to set up the antagonistic interaction gradient of the organizer molecules with BMP for epidermal and neural induction (Delaune et al., 2005). The use of FN in the interaction between BMP and its antagonists is a reason we have chose FN as our matrix for printing. However, after preliminary results show no difference between using fibrin or FN, fibrin was used for the rest of the experiments.

Aside from trying to replicate what is happening *in vivo*, the solid-phase approach allows for more extensive testing of the signaling molecules present in a developmental model. With liquid-phase assays, researchers were only able to test responses at a particular concentration. If they were assessing different responses due to different concentrations, they had to perform multiple assays, and then gather the results to describe the response a tissue has over a range of different concentrations. A solid-phase approach will not be limited to using only one concentration or one signaling molecule for each assay. With solid-phase signaling, we can set up concentration gradients to detect graded differentiation responses. Along with concentration gradients, we can set up competition assays between two or more signaling molecules. In the liquid-phase assays, this idea of a competition assay could only be set up at a particular concentration and with little control over the interactions between the signaling molecules.

VIII. Plan of Thesis

A. Rationale:

Cells become different in development due to induction, a ligand-mediated cell interaction. The conventional approach to induction with *Xenopus*, employs placing cells in a growth factor solution. This design misrepresents *in vivo* conditions. Here, I propose solid-phase induction as a more realistic and controllable approach. My objectives were: (1) To design a solid-phase induction chamber for presentation of growth factors, and (2) To inducing *Xenopus* animal caps to differentiate into mesoderm, via presentation of FGF-2 in solid-phase.

B. Experimental Approach:

I will present both the design of the solid-phase chamber as well as the results of solid-phase FGF-2 induction of *Xenopus* animal caps. Multiple membranes and grids were tested until the optimal chamber was obtained. Once the chamber was designed, *Xenopus* embryos were cultured to the desired stage of development, and animal caps were isolated. These caps were placed into liquid-phase cultures with FGF-2 in solution or into solid-phase chambers with FGF-2 attached to glass slides. Mesoderm gene expression was analyzed with RT-qPCR and *in situ* hybridization.

Material and Methods

I. *Xenopus* Embryos:

Sexually mature male and female frogs were purchased from *Xenopus* express (<http://www.xenopus.com>). These animals were fed and maintained in a colony until fertilization. Females were injected in their thigh, just under the skin with 0.05 ml 1 unit/ul Gonadotropin from pregnant mares' serum (PMS), as shown in Fig. 1, around 6:00 pm to initiate the ovulation procedure and stored at room temperature (Sigma). Two to three days later, the frogs were injected in the same place with 0.6 ml 10 units/ul Human Chorionic Gonadotropin (HCG) at 6:00 pm and placed in a 15°C incubator overnight (Sigma). Between 9 and 10 am the next morning, the female was removed from the incubator and placed at room temperature for 30 min. During this time a male frog was sacrificed and dissected to remove the testes. The testes were placed in 200% Steinberg's containing 1X gentamicin and stored at 4°C until needed. Two ml of 80% Steinberg's were placed in the center of a Petri dish and ¼ of a testis was minced to release the sperm. The female was then gently squeezed to aid in the release of her eggs. This dish, containing the 80% Steinberg's, sperm, and eggs, was gently swirled and left at room temperature for 5 min.

After this time, the Petri dish was flooded with 20% Steinberg's and left at room temperature. About 30-40 min post-fertilization, the solution was poured off and replaced with 2.5% L-cysteine HCl, pH 7.8, and continuously swirled until the jelly layer was removed (\approx 5 min). The embryos were washed 4-5 times with 20% Steinberg's, being careful not to allow the embryos to come in contact with the air/water interface. The embryos were then transferred to a new Petri dish containing fresh 20% Steinberg's

and allowed to develop at room temperature to stage 9 (newicop and fabor), Fig. 1, approximately 6 hours at 23°C. Once the embryos reached late blastula, they were dissected.

II. Animal cap isolation:

When the embryos reached stage 9, stage 8-10 for albino embryos, they are transferred to a Petri dish containing 100% Steinberg's and 1X gentamicin for dissection. Dissections were performed with the Gastromaster (Xenotek Engineering) using the yellow platinum tip set at a cutting diameter of 750 um and on the high yellow setting. The use of this machine allows for fast and precise dissections without the need to remove the fertilization membrane. Animal caps were isolated 12-15 at a time, and transferred with a plastic Pasteur pipette to a 6 well plate containing different concentrations of FGF-2 for liquid-phase induction or to the solid-phase chamber for solid-phase induction.

III. Liquid-phase induction:

To induce the isolated animal caps to differentiate via liquid-phase induction, all that is needed is the tissue, a 6 well culture plate, and the growth factor, in this case FGF-2. The 6 well plates were filled with 5 ml of 20% Steinberg's containing the desired concentration of FGF-2. One control well was filled, with 20% Steinberg's and no FGF-2. Once the plate was filled it was stored on ice while the isolation of the animal caps was being performed. Twelve to fifteen animal caps were transferred to each well and placed on a nutator for 4 hours. After 4 hours, the caps were transferred to individual 1.5

ml microcentrifuge tubes, which were submerged in liquid nitrogen. Once all of the caps were collected and frozen, the tubes were stored at -80°C for later use.

IV. Design of the solid-phase chamber:

a. Fibrin slide preparation:

Fibrin coated glass slides were prepared essentially as described by Miller et al. (Miller et al., 2006). Glass slides were cut into 1 in. squares. Glass was cleaned first with sulfuric acid and NOCHROMIX for 2 hours, rinse with deionized water ten times, and dried under nitrogen gas. Glass was then incubated in 95% acetone containing 1% 3-aminopropyltriethoxysilane (Gelest, Inc. Morrisville, PA) for ten min. at 23°C to coat glass surface with amine groups. Glass slides were then rinsed in acetone, ethanol, and deionized water respectively three times.

Squares were then dried at 120°C for 45 min. and then incubated in a 3% glutaraldehyde solution (Electron Microscopy Sciences, Hatfield, PA) in phosphate buffered saline, pH 7.4, at 37°C for 2 hours. Squares were then rinsed twice with methanol and then twice with deionized water.

Slides were then incubated in 0.1mg/ml fibrinogen (Aventis Behring, King of Prussia, PA) contained in 10 mM sodium phosphate buffer, pH 7.4 at 4°C for 18 hours. Excess fibrinogen was removed by aspiration and then remaining active sites on the glass slide was blocked with 0.3 M glycine (Bio-Rad Laboratories, Hercules, CA), pH 7.4 at 4°C for 2 hours. This was followed by 3 rinses with PBS. The fibrinogen was then converted into fibrin by incubation with 4 U/ml thrombin (Aventis Behring, King of Prussia, PA) contained in 10 mM sodium phosphate buffer and 1 mM calcium chloride

for 2 hours at 37⁰C. Slides were then rinsed with sterile deionized water twice, and the air-dried in a laminar flow hood. The thickness of the fibrin films was estimated to be approximately 20 nm, and it was verified that the glass slide was covered uniformly with a transmission and scanning electron microscope. FN coated slides were prepared the same way with the FN added to the fibrin.

b. Solid-phase induction:

The fibrin slides that were stored in PBS were transferred to fresh Petri dishes inside a sterile hood and washed twice with sterile water. The slides were placed on a Kimwipe and allowed to dry for 30 min. Once dry, a desired amount of FGF-2 was spotted onto the center of the slide and allowed to adhere and dry for 30-45 min. After the FGF-2 was dry, the outline of the spot was scored with a diamond tip pen and the slide was placed in 4⁰C submerged in 100% Steinberg's at 4⁰C overnight.

A medium Petri dish (60 x 15 mm) was taken, and four corners of a 1 cm square were spotted with machine grease in the center of the Petri dish. A 1 cm square of NYTRAN Plus paper was cut as well as a 1 cm square of stainless steel grid (DexMet; Brandford, Conn.). Once everything was prepared, the fibrin slides were removed from the refrigerator and stored on ice until they were used. The Petri dish was filled with 20% Steinberg's and the NYTRAN paper was placed under the grease spots. Next the stainless steel grid was lowered on top of the grease spots and firmly pressed down with forceps. Once the chamber was set up, the animal caps were isolated and transferred to the grid with a plastic Pasture pipette. The animal caps were manipulated with fine forceps with the outer layer of cells lying on the NYTRAN paper. Once 8-10 animal caps were centered in the grid, the fibrin slide was laid on top of the grid, fibrin side

down, with the FGF-2 centered over the animal caps. To ensure good contact between the animal caps and the FGF-2, 5 mechanical washers (diameter 1 ½ cm) were taped together and lowered on top to the glass slide. This setup was performed in 20% Steinberg's. The chamber was allowed to sit at room temperature for 4 hours at which time the animal caps were transferred to fresh 1.5 ml microfuge tubes. A pipette was used to remove as much Steinberg's as possible, without letting the animal caps come in contact with the air/water interface, and then the caps were submerged in liquid nitrogen. Once all caps were frozen, the microfuge tubes were transferred to -80° until later use.

V. RNA extraction:

Once a sufficient number of animal caps were induced and collected for RT-qPCR, RNA was extracted using the RNeasy Mini Kit (Qiagen). Prior to isolation, 10 ul β -Mercaptoethanol (β -ME) was added per 1 ml Buffer RLT. This solution was reused in subsequent extractions for up to 1 month. Caps were removed from -80°C and 350 ul of β -ME + Buffer RLT was added, on ice, before samples thawed. Samples were mixed by pipetting and transferred to a QIAshredder column (Qiagen), placed in a fresh 1.5 ml microcentrifuge tube. The sample was centrifuged for 3 min, and the supernatant was transferred to a fresh 1.5 ml microcentrifuge tube, to which 350 ul of 70% ethanol was immediately added and mixed with gentle pipetting. The sample was transferred to an RNeasy mini column (Qiagen) that was placed into a 2 ml collection tube, and centrifuged for 15 sec. The flow-through was discarded and 700 ul of buffer RW1 was added to the RNeasy column and centrifuged for 15 sec. Once again the flow-through was discarded and the RNeasy mini column was transferred to a fresh 2 ml collection

tube. Next, 500 ul of buffer RPE was added to the column and centrifuged for 15 sec, discarding the flow-through. This step was repeated again, but the sample was centrifuged for 2 min. The dry RNeasy mini column was transferred to a fresh 1.5 ml microcentrifuge tube where 30 ul RNase-free water (MP Biomedicals: Irvine, CA) was added directly to the membrane and centrifuged for 1 min. The flow through now contains the purified RNA which was then stored at -80°C for later use.

VI. RT-qPCR:

a. 1 step RT-qPCR amplification:

After RNA extraction, real-time RT-qPCR reactions were performed using One-Step Taqman[®] RT-PCR Master Mix, primers and probes (Applied Biosystems: Foster City, CA. and IDT). The *Xenopus* primer and probe sequences were as follows: *Xbra*. forward- 5' CAC CTC ACT ACT CGT CTC TTT CAC A 3'(IDT# 17959291), reverse- 5' TGC TCC ATG CTC ATA CAA TGG 3'(IDT# 17959292), probe- 5' TGT GCC CTC ACC ATC CAC AGG ATC 3' (IDT# 17959294); *Xwnt-8*. forward- 5' GCT ACC CAC AAT GGA CTT CGA 3', reverse- 5' AAC TCC CGC TGA GCT AAT GG 3', probe- 5' TGC AAC CAG AGA AAC CTC CTT TGT; 18S primers and probes were designed by Applied Biosystems (Foster City, CA) and the sequences were not given. The 18S primers and probes were designed for human DNA amplification but could be used for *Xenopus* as well, as stated by Applied Biosystems (Foster City, CA). Both *Xbra* and *Xwnt-8* probes were labeled with a 5' FAM reporter dye and a 3' TAMRA quencher dye. The 18S probe was labeled with a 5' VIC reporter dye and a 3' TAMRA quencher dye.

Two ul of RNA sample was used per 10 ul reaction with One-Step Taqman RT-PCR Master Mix (Applied Biosystems: Foster City, CA), sequence specific primers (50nM), and Taqman Probes (100nM). A master mixture of all components except for the RNA was added together with the following components per sample of RNA: 24 ul Taqman One-Step Master Mix (2X), 18.96 ul RNase free water, 0.96 ul Forward primer (10 uM), 0.96 ul Reverse primer (10 uM), 0.96 ul Probe (5uM), 1.2 ul RT/RNase Inhibitor (40X), and a total volume of 48 ul was reached with RNase free water. From this master mix, 38 ul was removed and put into a new microfuge tube to which 2 ul of sample RNA was added. The tube was vortex and 10 ul was removed and dispensed into a well of the PCR plate. Real-time RT-qPCR assays were carried out in triplicate using an ABI Prism 7900 Sequence Detection System (AME Bioscience). The thermocycling conditions were as follows; 48°C for 30 min (reverse transcription), 95°C for 10 min (initial denaturation) followed by 40 cycles at 95°C for 15 sec (denaturation) and 60°C for 45 sec (annealing and extension).

b. Separation and analysis of data:

Once the real-time RT-qPCR reactions were complete, the data was analyzed by using the sequence detection system (SDS) program version 2.1. The threshold was set above the non-template control within the linear phase of the target gene amplification to calculate the cycle number at which the transcript is detected (C_T). The ribosomal gene 18S was used as the reference to normalize the target gene expression. Validation experiments conducted previously demonstrated that efficiencies of target genes and reference genes were approximately equal with the absolute value of the slope of log

input amounts vs. $\Delta C_T < 0.1$ (J. Jowdlic, Carnegie Mellon University). Total RNA in each sample was determined by the ΔC_T values of the control groups (18S). To be able to calculate the fold differences of the target genes (Xbra and Xwnt-8) from the controls (18S), the comparative $\Delta\Delta C_T$ method was used as detailed in Applied Biosystems Bulletin #2 (37). For this analysis cycle numbers not detected were set at 40 cycles, the maximum cycle number, to allow for statistical analysis. Once the data was collected, it was entered into an excel document and used to produce the graphs seen in the results.

VII. *In situ* hybridization of animal caps:

a. Fixing caps for *in situ*:

In addition to RT-qPCR, *in situ* hybridization was used to examine Xbra expression in animal caps. Animal caps were dissected and induced/non-induced as described before and then transferred to a 5ml glass vial containing MEMFA. This fixative was prepared fresh each time and consists of 100 mM MOPS pH 7.0, 2 mM EGTA, 1 mM $MgSO_4$ and 3.7% formaldehyde. The vials were completely filled with MEMFA, and the animal caps were rocked horizontally on a nutator. After three hours, the vials were filled with fresh MEMFA and rocked horizontally for one hour. The vials were then filled with 100% ethanol, and rocked for five min. The ethanol was changed, and the vials were stored at $-20^\circ C$ until further use.

b. Xbra Plasmid Midi Prep:

A glycerol stock of Xbra plasmid was thawed on ice and then aseptically streaked onto a fresh LB/amp^r agarose plate. The plate was placed in a $37^\circ C$ incubator overnight. One colony was removed from the plate and placed into a fresh 70 ml beaker containing

50 ml LB/amp^r liquid agarose. The beaker was sealed with aluminum foil and placed in a shaking incubator at 37°C overnight. Fifty ml of the culture was transferred to a 50 ml polypropylene centrifuge tube and spun for 20 min at room temperature. Supernatant was discarded carefully so as not to disturb the pellet. The pellet was completely re-suspended in 4 ml of ice cold solution 1 (Eppendorf) and incubated at room temperature for 10 min, and on ice for an additional 5 min. Solution 2 was added, and the tube was mixed by inversion to lyse the bacteria and placed on ice for 5 min. After lysis, 4 ml of solution 3 was added. The tube was mixed by inversion, incubated on ice for 10 min and centrifuged for 25 min. The supernatant was removed carefully, without disturbing the pellet, and transferred to a fresh 50 ml centrifuge tube. To this solution, 10 ul of cold DNA Binding Matrix (Eppendorf) was added and mixed vigorously by vortexing. A spin column (Eppendorf) was placed into a fresh 50 ml centrifuge tube to which the solution was added and centrifuged for 10 min. The filtrate was discarded; and the remaining “cake” on the spin column was washed twice with the Purification mix (Eppendorf) by centrifugation for 5 min. After the second wash, the spin column was left at room temperature for 5 min to dry. Three ml of DEPC-water was added, and the tube was centrifuged for 5 min to remove the purified plasmid. A good yield was shown through spectrophotometry, and aliquots were distributed into 1.5 ml microcentrifuge tubes.

c. Restriction digest of Xbra Plasmid:

The digestion reaction was prepared by adding 10 ug of plasmid DNA, 20 ul restriction buffer, 10 ul restriction enzyme and DEPC-water to a final volume of 200 ul. This solution was incubated in a 37°C water bath for 4 hours. To terminate the reaction, 3 ul of 1 mg/ml proteinase K and 10 ul SDS were added and incubated in a 55°C water

bath for 45 min. Equal volumes of phenol: chloroform were added and vortexed to ensure absolute mixing of the solution. After centrifugation for 10 min, the top layer was carefully removed and transferred to a new microcentrifuge tube. An equal volume of chloroform was added to the mixture and centrifuged for 10 min. The top layer was once again carefully removed and transferred to a new microfuge tube. To the top layer, 20 ul 3M sodium acetate pH 5.2 and 500 ul ice cold 100% ethanol were added and left at -20°C overnight. The next day, the solution was centrifuged for 10 min, and the supernatant was discarded. The pellet was then washed twice with 70% ethanol. After the final wash, the pellet was allowed to air dry at room temperature for 25 min. Once the pellet was dry, it was re-suspended in DEPC-water and quantified with spectrophotometry. If the pellet did not re-suspend, the microfuge tubes were placed in a hot plate at 75°C for 5 min to aid in the re-suspension. The final suspension was stored at -20°C for later use.

d. Transcription of the sense and antisense probes:

The digested plasmid was used as the template for transcription of the sense and antisense probes. The transcription reaction was prepared at room temperature in a 1.5 ml microcentrifuge tube in the following order: 4 ul 5X transcription buffer, 2 ul 2X DIG RNA labeling mix (Roche: Indianapolis, IN), 1 ul 100mM DTT (Fisher), 1 ul RNase inhibitor (Takara: Madison, WI), 2 ul RNA polymerase SP6 for the sense strand (Invitrogen), or T7 (Fisher) for the antisense strand, 2 ug template, and DEPC-water to a final volume of 20ul. The mixture was incubated in a hybridization oven at 37°C for 3 hours. Once the reaction was complete, 1 ul was removed and run on an ethidium bromide gel to check for proper transcription. An equal volume of 8M LiCl was added to the rest of the reaction and stored overnight at -20°C. The next morning the solution was

centrifuged for 10 min, and the supernatant was discarded. The pellet was washed with 70% ethanol and allowed to air dry for 25 min. Once dry, the pellet was re-suspended in 100 ul DEPC-water and quantified with spectrophotometry. The transcript was hydrolyzed by adding 100 ul 80 mM sodium bicarbonate and 100 ul 120 mM sodium carbonate and incubating in a hybridization oven at 60°C for 30 min. After incubation was complete, 12.5 ul 8M LiCl and 500 ul 100% ethanol was added and placed at -20°C overnight. The solution was centrifuged for 5 min, and the pellet was washed twice with 70% ethanol and allowed to air dry for 25 min. The pellet was re-suspended in hybridization buffer and the amount of remaining probe was approximated by using the spectrophotometry reading taken just before hydrolysis.

e. *In situ* hybridization:

Animal caps that were fixed in MEMFA were transferred to fresh 5 ml glass vials filled with 100% ethanol for *in situ* hybridization. All subsequent washes and transfers were performed with plastic Pasteur pipettes. Each *in situ* procedure was carried out in four vials of animal caps, each with 3-4 animal caps: 1) animal caps treated with 100 ng FGF-2 and subjected to the antisense probe, 2) animal caps treated with 100 ng FGF-2 and subjected to the sense probe, 3) animal caps cultured in the solid-phase chamber without FGF-2 subjected to the antisense probe, 4) animal caps cultured in the solid-phase chamber without FGF-2 subjected to the sense probe. The vials went through an initial re-hydration procedure with the following washes performed in order: 100% ethanol, 75% ethanol + 25% DEPC-water, 50% ethanol + 50% DEPC-water, 25% ethanol + 75% PTw (1X PBS + 0.1% tween-20 (Fisher)), and 100% PTw for 5 min each while rocking on a nutator vertically. All subsequent washes were performed at room

temperature while rocking the vials vertically on a nutator unless stated otherwise. After re-hydration, caps were washed three times in 100% PTw for 5 min. The solution was replaced with 1 ml of 10 ug/ml proteinase K and incubated for 10 min. The caps were washed twice with 5 ml 0.1 M triethanolamine pH 7.5 for 5 min each. To the second wash 12.5 ul acetic anhydride (Sigma) was added and incubated for 5 min at which time an additional 12.5 ul acetic anhydride was add for 5 more min. Caps were washed three times in 100% PTw for 5 min each and refixed in 4% paraformaldehyde for 20 min. Stock 20% paraformaldehyde was prepared in H₂O and the cloudiness was neutralized with NaOH while mixing on a hot plate at 65°C. Mixing was ceased after solution was clear, and the solution was covered in foil and stored at 4°C. Once fixed, the caps were washed three times in 100% PTw for 5 min each. All but one ml of the PTw was removed and 250 ul of hybridization buffer was added and allowed to settle to the bottom of the vials for 5 min. This was replaced with 500 ul of fresh hybridization buffer and incubated in a hybridization oven for 10 min at 60°C. The solution was once again replaced with a fresh 500 ul hybridization buffer and incubated at 60°C in the hybridization oven for 4 hours for pre-hybridization. After pre-hybridization, the solution was replaced by 500 ul of fresh hybridization buffer containing 1 ug/ml of either the sense or antisense probe and incubated overnight in the hybridization oven at 60°C. The next day the caps were washed for 10 min with 500 ul fresh hybridization buffer at 60°C in the hybridization oven. Three successive washes were performed with 2X SSC for 20 min each at 60°C in the hybridization oven. Caps were RNase treated with a wash containing 5 ml of 2X SSC with 20 ug/ml RNase A (Sigma) and 10 units/ml RNase T₁ (Sigma) for 30 min at 37°C in the hybridization oven. The RNase treatment was

followed with two washes with 0.2X SSC for 30 min each at 60°C in the hybridization oven. This solution was replaced with Maleic acid buffer (MAB: 100 mM Maleic acid, 150 mM NaCl, pH 7.5) twice for 5 min each at room temperature. The caps were washed with 2% Boehringer Blocking reagent (BMB, Roche) in MAB for one hour at room temperature. This solution was replaced with 500 ul MAB + 2% BMB + 20% heat treated lamb serum (Gibco) for one hour at room temperature. Antibody addition was performed by adding 500 ul fresh MAB + 2% BMB + 20% heat treated lamb serum and 0.25ul antidigoxigenin antibody coupled to alkaline phosphatase (Roche) and incubated at room temperature for 4 hours. After incubation, any unbound antibody was washed away five times, for one hour each, with fresh MAB. One of these washes was performed overnight at 4°C. To prepare the caps for visualization of the chromogenic reaction, they were washed in 5 ml of freshly made alkaline phosphatase buffer (100 mM Tris, pH 9.5, 50 mM MgCl₂, 100 mM NaCl) twice for 5 min each. This solution was replaced with 500 ul BM purple staining reagent (Roche) and rocked vertically in a closed box on a nutator until sufficient staining could be seen. Staining was checked either by viewing through the glass vials or by transferring the caps into a Petri dish containing fresh alkaline phosphatase buffer. The BM purple staining reagent was replaced if precipitate was forming. Times for sufficient staining ranged from 3 ½ hours to 4 ½ hours during these experiments. Once satisfied with the staining, the caps were fixed in MEMFA for 3 hours, followed by two washes in 100% ethanol. Caps were transferred to Petri dishes containing 100% ethanol for photography, and stored in 100% ethanol at -20°C.

f. Photography of animal caps:

Once the *in situ* procedure was complete the caps were transferred to Petri dishes containing 100% ethanol. Sense and antisense stained caps were photographed with a digital camera (Q-imaging Corporation) attached to a dissecting microscope. Caps were carefully manipulated and moved with a fine hair loop while always keeping the caps submerged in the 100% ethanol. Pictures were taken with a red transparent film underneath the Petri dishes for better contrast. All pictures were formatted with Adobe Photoshop.

Results

I. Liquid-phase FGF-2 induction:

Reverse Transcription-Polymerase Chain Reaction (RT-PCR) was used to detect *Xbra* transcripts in FGF-2 induced *Xenopus laevis* animal caps. Primers were designed using Primer Design 2.0. A set of primers forward and reverse were returned of which one forward and one reverse primer were picked to amplify the transcript as indicated in Material and Methods. *EF1- α* , which is expressed throughout the embryo as a “housekeeper” gene, was used as a positive control for the RT-PCR reactions. A band was expected when using the *EF1- α* primers to indicate good cDNA synthesis from the total RNA extracted (Fig.4). A negative control was also included, not indicated in the figures, where RNA was used as the template with the *EF1- α* primers instead of cDNA.

Xbra was expressed in whole embryos as well as was animal caps that were induced with FGF-2 (Fig. 4). Animal caps that were isolated at the same stage but cultured in 20% Steinberg’s showed no *Xbra* expression (Fig. 4).

II. Solid-phase chamber design:

The design of the solid-phase chamber entailed a few requirements for proper presentation of the growth factors to the isolated animal caps. The animal caps had to remain flat to allow the inner cells to be exposed to the solid-phase growth factors. The caps had to also be secluded from one another to inhibit signaling from one cap to the other.

Isolated animal caps heal around themselves once removed from the embryo. What this means is the outside of the cap acts as a wound that heals rapidly by rounding up into

a sphere, with the outer surface of the cap enveloping the inner cells (Kofron 2002). A method had to be employed to control the movements of these animal caps to allow for induction. Different types of nitrocellulose papers and membranes were tested for adherence of the pigmented outer layer of the isolated animal caps. Isolated animal caps from late blastula embryos were healed 30 min post-dissection in the absence of NYTRAN paper (Fig. 5A). This is shown by the pigmented outer layer completely enveloping the cap (Fig. 5A). Isolated animal caps, also from late blastula embryos, that were placed pigmented side down onto NYTRAN Plus nitrocellulose paper showed no evidence of healing with the inner cells remaining exposed to the surrounding solution 45 min post-dissection (Fig. 5B).

Once the healing of the animal caps was inhibited, the next step was to isolate the individual caps from one another, and control the contact of the solid-phase glass slide. The rest of the chamber provided this control by utilizing a stainless steel grid, 700 μm in pore diameter and 100 μm in depth (Fig. 6A+B). The third component of the chamber was the Fibrin coated glass slide. The slide was the site for FGF-2 attachment, and was placed directly on top of the stainless steel grid (Fig. 6B). The final component of the solid-phase chamber was a set of washers taped together, and placed onto the glass slide for added weight (Fig. 6C).

III. Establishing an RT-qPCR assay for transcript detection:

Solid-phase induction of animal caps was assayed by employing RT-qPCR to quantitatively detect levels of *Xbra* expression. *Xbra* primers and probes were designed

using Primer Design 2.0 as stated in Material and Methods. 18S human primers and probes (Applied Biosystems) were used as directed by ABI.

18S is expressed throughout the embryo, and is used in RT-qPCR experiments as the control for RNA detection as well as a control to normalize the amount of experimental transcript present.

IV. RT-qPCR detection of *Xbra* in liquid-phase and solid-phase FGF-2 induction:

Xbra expression was detected in RT-PCR of liquid phase FGF-2 induction so it was important that this same result could be shown employing the new method, RT-qPCR. The results indicated that with increasing concentrations of FGF-2, there was an increase in *Xbra* expression (Fig. 7A). In the absence of FGF-2, there was no expression of *Xbra* (Fig. 7A).

Solid-phase induction was initiated by isolating stage 9 (Newikop and Faber) animal caps and exposing them to the solid-phase FGF-2 for four hours to allow for mesoderm induction. The concentrations used were determined by the results seen with MG-63 cells (Campbell 2005). The results indicate an increase in *Xbra* expression in relation to an increase in FGF-2 presented to the animal caps in the Solid-phase chamber (Fig. 7B,C,D). In the solid-phase induction experiments there were two negative controls used per RT-qPCR run. The first control was the placement of the animal caps in 20% Steinberg's without the presence of FGF-2 or the solid-phase chamber. The second control was also in the absence of FGF-2 but caps were cultured in the Solid-phase chamber to simulate the mechanical stress induced by being in the chamber. In all of the

experiments performed there was little or no expression of *Xbra* in both of the negative controls (Fig. 7).

Each one of the points represented on the graph indicates a single RNA sample extracted from 6-8 animal caps that came from the same female and were induced in the same solid-phase chamber separate from all other samples. Each graph represents separate RT-qPCR experiments performed with different RNA, master mixes, and in a different 384 well plate. Although they each individually showed quantitatively different results, they all showed the same trend of increasing *Xbra* expression with an increase of FGF-2 presented.

The values represented on the graph for the solid-phase FGF-2 induction represent the mass amount of FGF-2 applied to the Fibrin coated glass slide. Each animal cap had a surface area of $384,845.1 \mu\text{m}^2$, the 5ng, 50ng mass amount used a 5ul spot of FGF-2 which had a surface area of $7,068,583.5 \mu\text{m}^2$ and, the 10ng, 100ng mass amount used a 10ul spot of FGF-2 which had a surface area of $12,566,370.6 \mu\text{m}^2$. Using a ratio of these surface areas, the approximate mass amount of FGF-2 presented to each animal cap at 5ng was .27ng, at 10ng was .31ng, at 50ng was 2.7ng, and at 100ng was 3.1ng.

V. *In situ* hybridization of animal caps induced with FGF-2:

In situ hybridization was performed on the animal caps to confirm the results seen with RT-qPCR and to visualize any pattern of *Xbra* expression. Animal caps were grouped into 4 different categories:

- 1) FGF-2 induced animal caps with the antisense probe
- 2) FGF-2 induced animal caps with the sense probe

3) Non-induced animal caps with the antisense probe

4) Non-induced animal caps with the sense probe

Three experiments were performed with two independently synthesized sense and antisense probes. They were also performed on different batches of animal caps from embryos originating from different females and males. Two of the three experiments showed similar staining patterns (Fig. 8A+B), while the third showed no staining (not shown). The lack of staining in the third experiment was due to the inability to continue the staining step to completion.

In both experiments, all seven animal caps that were induced with FGF-2 and exposed to the antisense probe showed staining throughout the animal caps (Fig. 8A,B)

Conversely, in both experiments all seven animal caps that were induced with FGF-2 and exposed to the sense probe exhibited no staining (Fig. 8A,B). Also, in both experiments all six of the animal caps that were not induced with FGF-2 and exposed to the antisense probe showed no staining (Fig. 8A,B). In both experiments all five animal caps that were not induced with FGF-2 and exposed to the sense probe showed no staining (not shown).

Fig. 3: Animal cap isolation

Xenopus embryos were allowed to develop to late blastula-early gastrula, stage 9. At this point the animal cap was excised with the Gastromaster dissection tool as indicated.

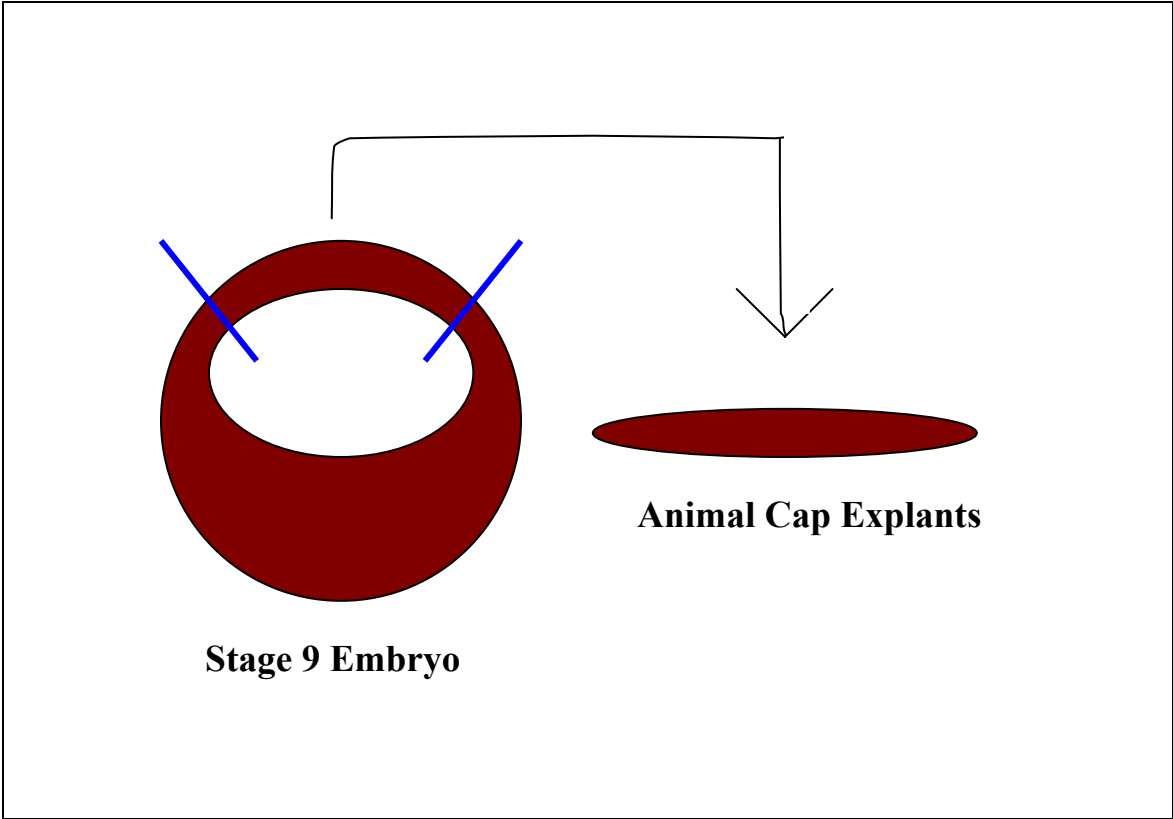


Fig. 3

Fig. 4: Expression of the mesoderm marker Xbra in response to FGF-2 in liquid-phase.

Three cDNA samples were analyzed: 1) animal caps treated with FGF-2 at 10 mg/ml (+), whole embryos (w), and untreated animal caps (-). The top six lanes represent RT-PCR with primers for the constitutively expressed gene EF1- α , the bottom six lanes represent RT-PCR with primers for the mesoderm marker Xbra. Experiments were done in duplicates.

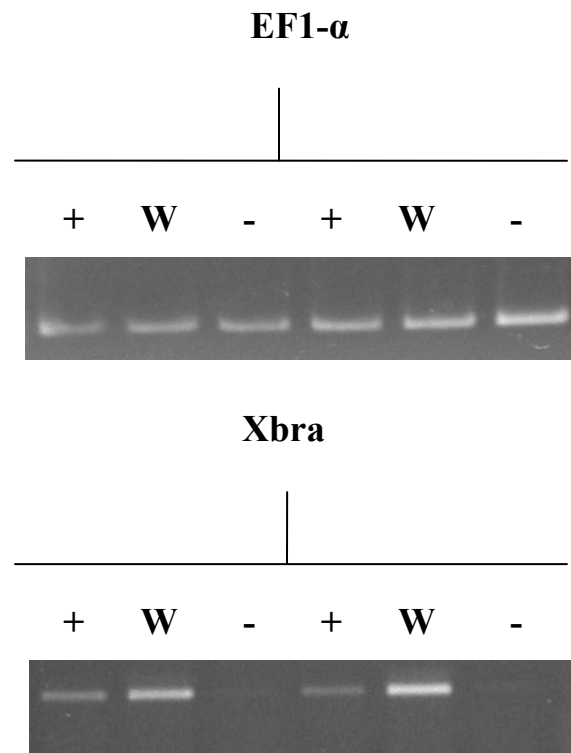


Fig. 4

Fig. 5: Inhibition of animal cap healing

(A) Isolated animal caps undergo wound healing. The outer pigmented cell layer migrates around the inner cells forming a sphere, isolating the inner cell from the surrounding media. This process will take place within 20 min post-dissection (Bar = 200 um). (B) Animal caps that are placed, pigmented side down, on NYTRAN nitrocellulose paper remain un-healed 45 min post-dissection (Bar = 700 um)

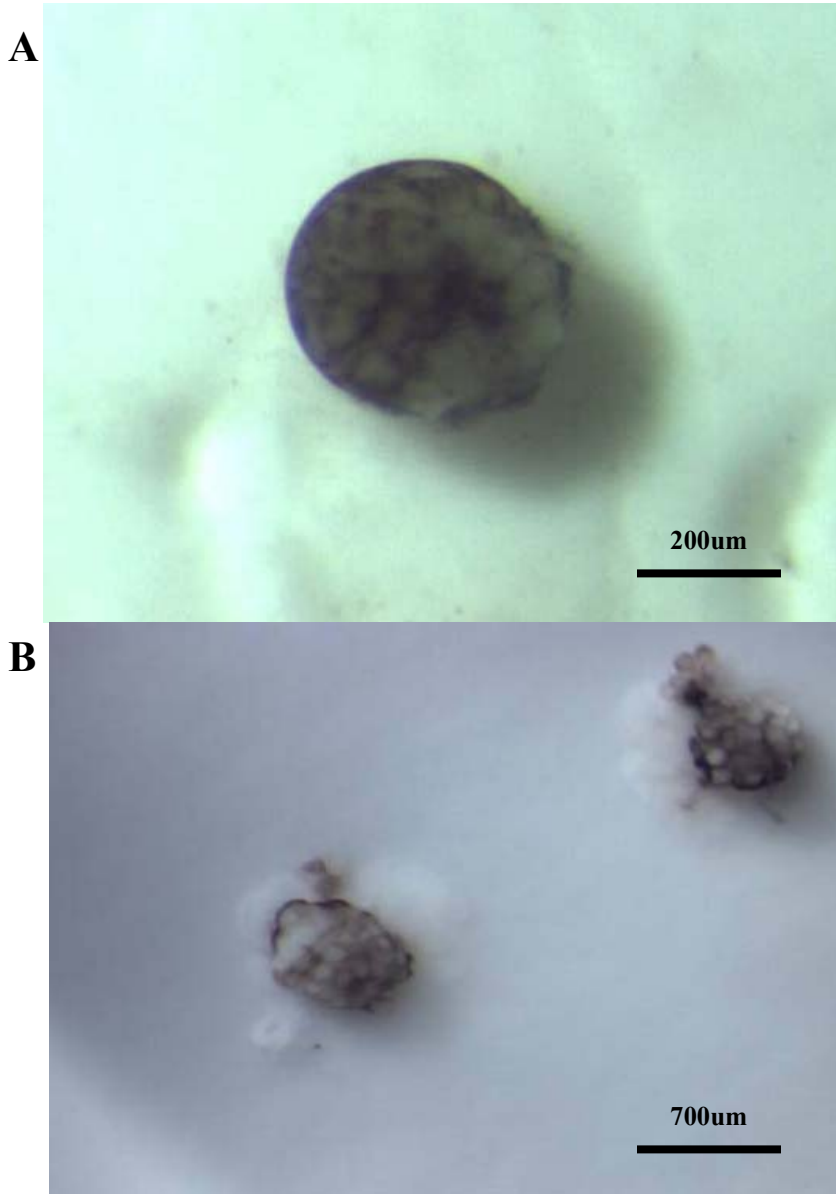
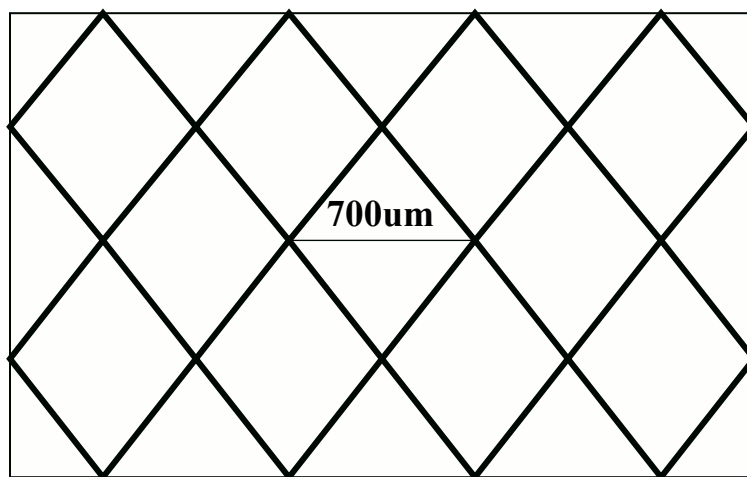


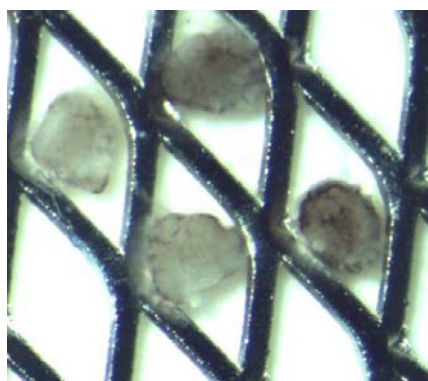
Fig. 5

Fig. 6: Solid-phase chamber design

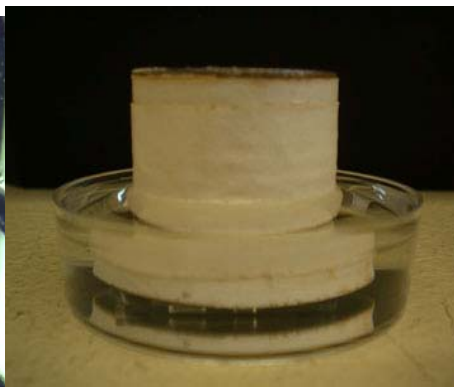
(A) The stainless steel grid used in this design was 100um thick and the pore openings had a width of 700um as indicated. (B) This grid was laid onto the nitrocellulose membrane, at which time the animal caps were placed into the openings. The glass slide containing the solid-phase FGF-2 was then placed on top. (C) The final component of the chamber, the washers, added the necessary weight to maintain the contact between the glass slide and the animal caps.



A



B



C

Fig. 6

Fig. 7: Xbra expression in response to FGF-2, presented in liquid-phase or solid-phase

Each point on the graph indicates a single RNA sample extracted from 6-8 animal caps from the same female. In the solid-phase cases (B,C,D), the 6-8 caps were induced in the same solid-phase chamber separate from all other samples. Each graph represents a separate RT-qPCR experiment performed with different RNA, master mixes, and 384 well plate. (A) The log fold expression of Xbra over the control in response to liquid-phase presentation of different concentrations of FGF-2. (B,C,D) The log fold expression of Xbra over the control in response to solid-phase presentation of different concentrations of FGF-2. (-) control represents animal caps cultured in 20% Steinberg's with no FGF-2. 0ng/ul:5ul represents the second control where animal caps were cultured in the solid-phase chamber in the absence of FGF-2. The values indicated on the graph represent the mass amount of FGF-2 applied to the Fibrin coated slide. The approximate amount of FGF-2 presented to each animal cap for each mass amount used is shown in the results text.

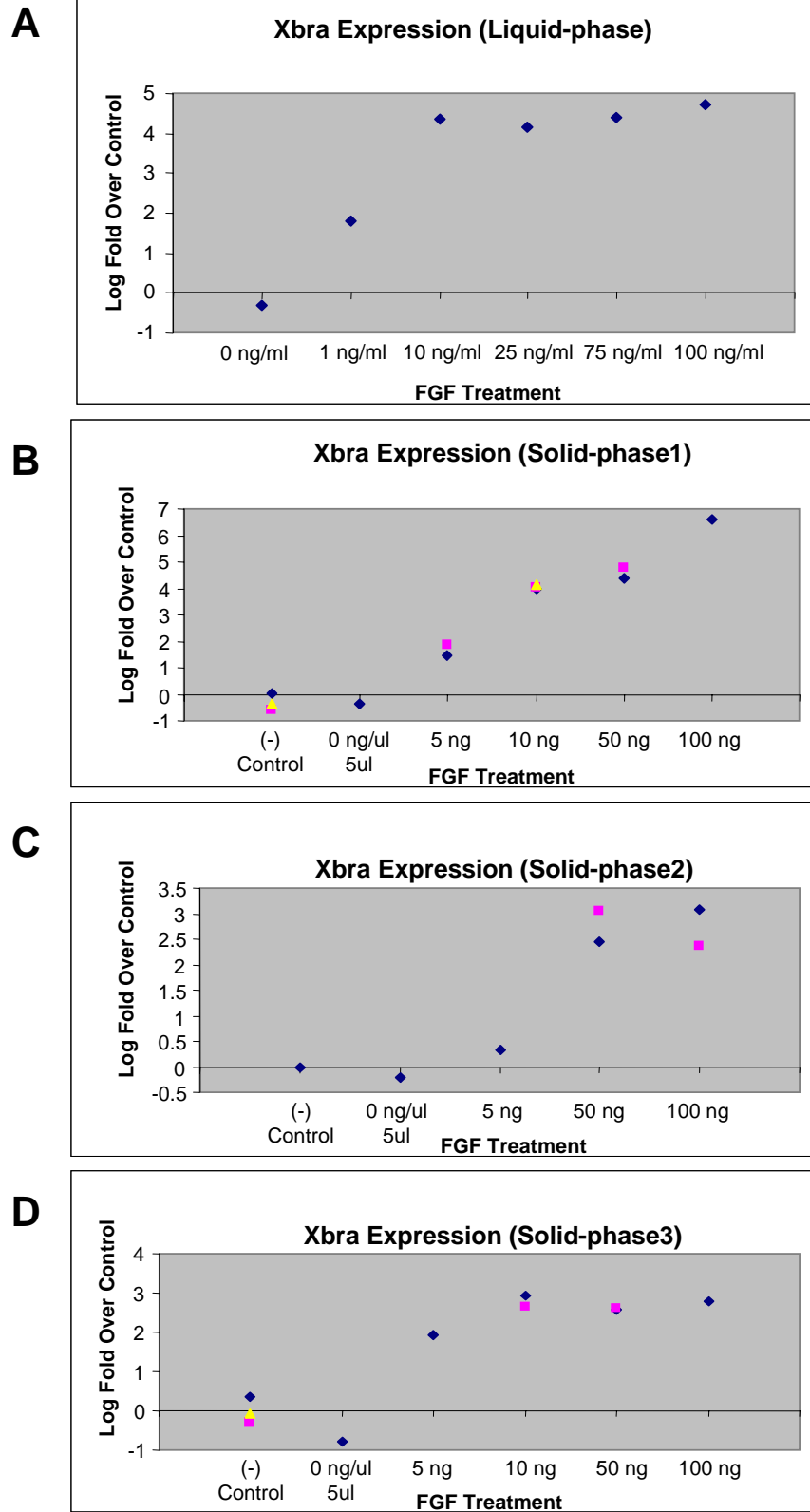
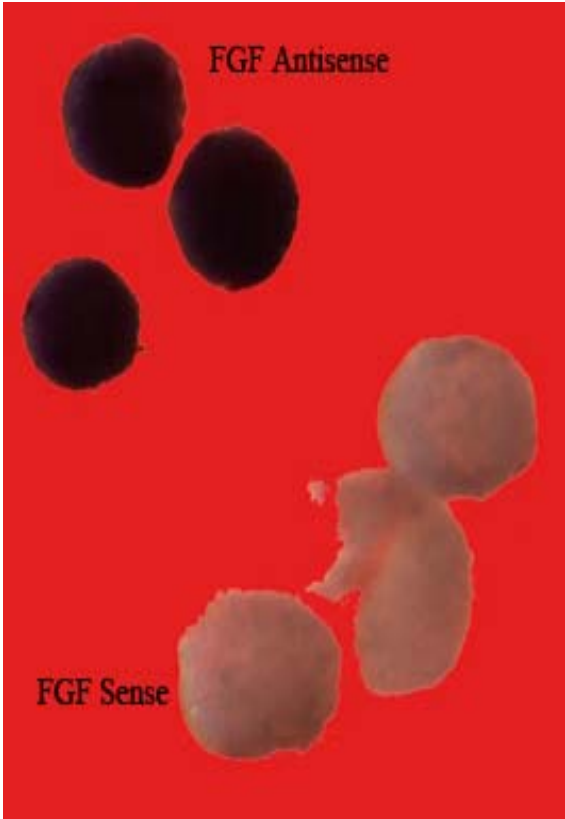


Fig. 7

Fig. 8: *In situ* of animal caps exposed to FGF-2

(A) *In situ* hybridization was performed with sense and antisense Xbra probes on animal caps that were treated with solid-phase FGF-2 and animal caps that were untreated. The untreated caps were allowed to develop for the same amount of time as the treated caps inside the solid-phase chamber. (a) Animal caps that were treated with solid-phase FGF-2 and incubated with the Xbra antisense probe showed dark staining throughout the cap (FGF Antisense). As expected, caps that were treated with solid-phase FGF-2 and incubated with the Xbra sense probe showed no staining (FGF Sense). (b) Animal caps that were left untreated and incubated with the Xbra antisense probe showed no staining (Untreated Antisense). (B) *In situ* experiment two. Same results seen as in A but with lighter staining.

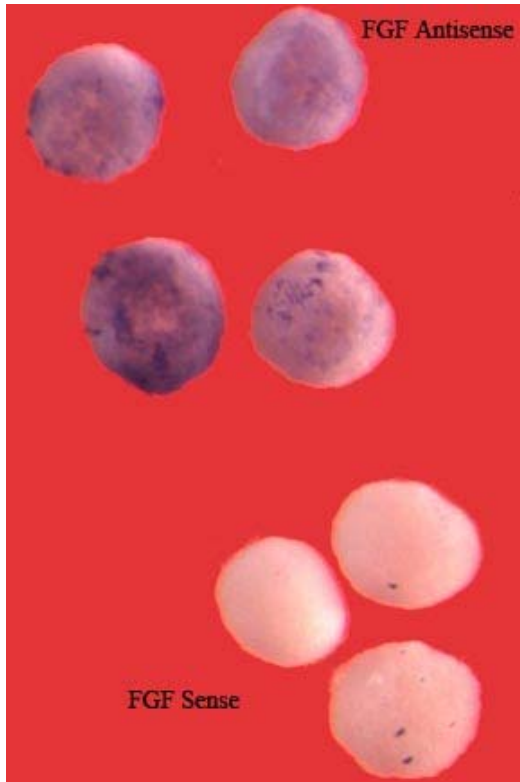


a

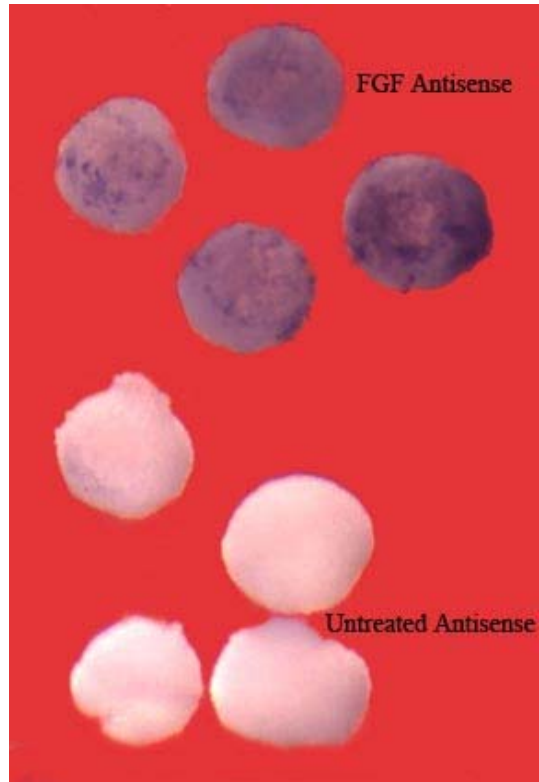


B

Fig. 8A



A



B

Fig. 8B

Fig. 9: New solid-phase chamber design

The new solid-phase chamber is composed of de-ionized aluminum. (A) The dimensions of the grid will be the same as in figure 7 with a thickness of 100 μm and the pore width being 700 μm . The grid insert contains 16 pores for animal cap placement, as well as grooves cut on the underside to allow for exposure of the caps to oxygen. (B) The chamber will utilize two screws for correct placement of the solid-phase growth factor containing glass slide. These screws will also apply the correct weight necessary for constant contact between the glass slide and the animal caps (drawing not to scale).

New Design Layout

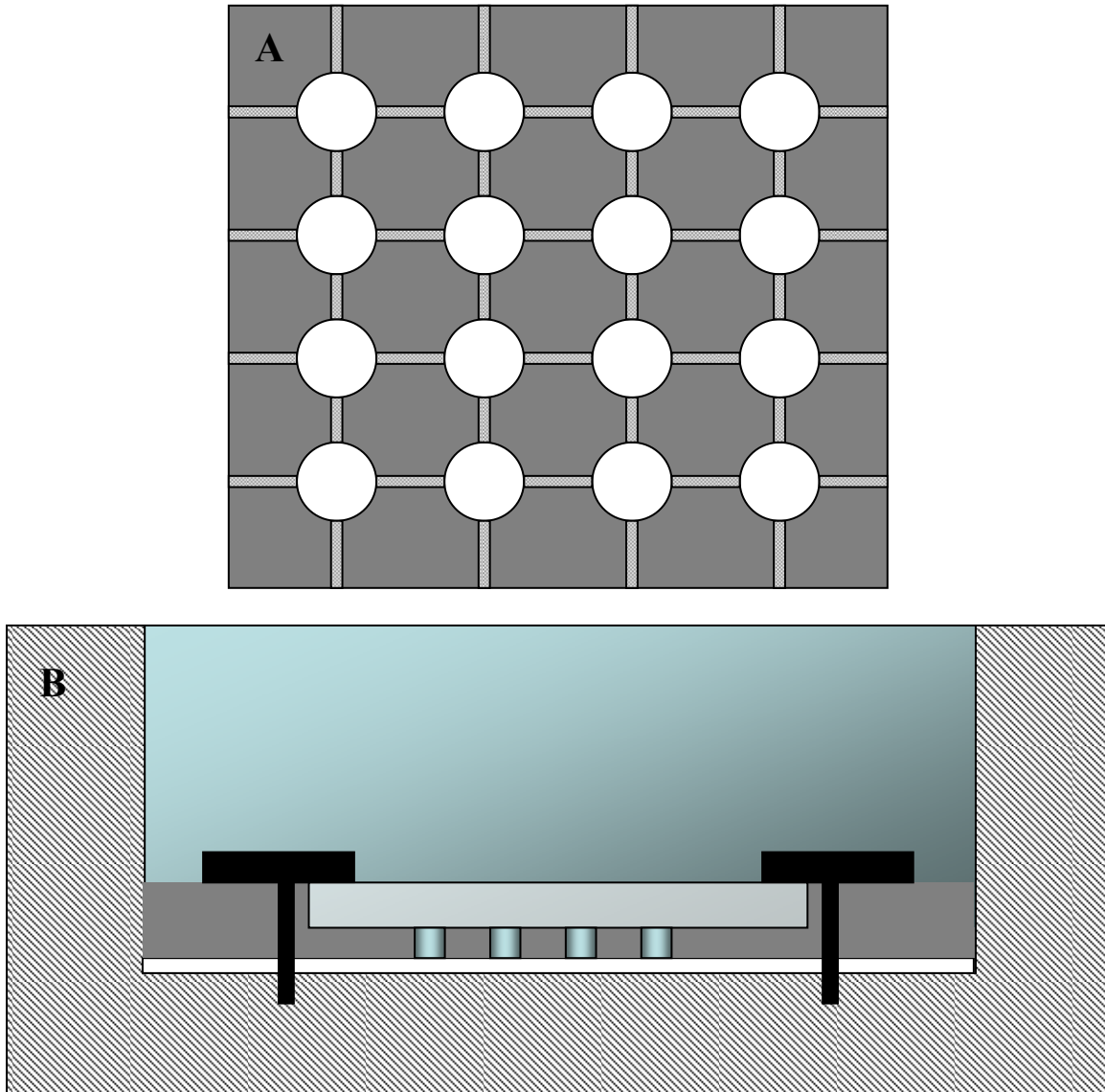
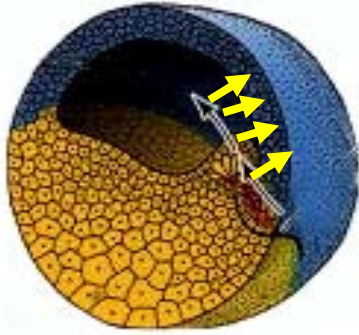


Fig. 9

Fig. 10: Model for neural induction experiment

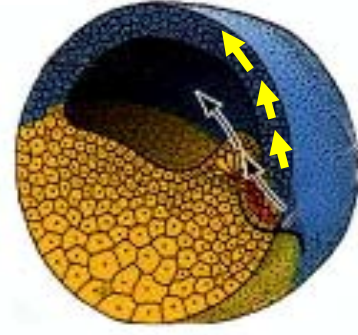
(A) The two current, models for neural induction by the organizer tissue are indicated by the two drawings. The vertical hypothesis states that as the organizer passes underneath the ectoderm the vertical release of the inhibitor molecules induce neural tissue. On the other hand, the horizontal hypothesis states that there is a single, initial release of inhibitor molecules at the dorsal lip that propagates through the ectoderm. (B) This can be directly tested with the application of the solid-phase approach, and the printed pattern of noggin indicated. (C) The two possible results that would be expected after performing *in situ* on the animal caps, in relation to the type of induction taking place are as indicated. If the vertical mode is correct, the staining should only be present where the animal cap was in contact with the noggin. If the horizontal mode is correct, a diffuse staining should be seen within the contact area as well as further around. (Fig. 10.7 from Gilbert, 2000 was used for this figure by permission from Sinauer Inc).

A



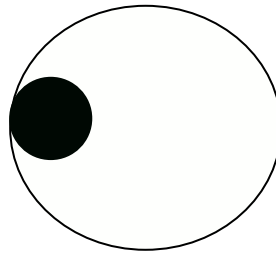
Vertical

A



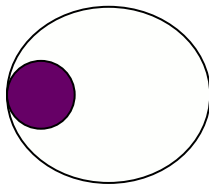
Horizontal

B

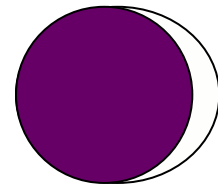


Pattern

C



C



In situ result

Fig. 10

Discussion

I. Liquid-phase induction with FGF-2:

Initial liquid-phase induction with FGF-2 shows expected results with RT-PCR analysis. Animal caps that were cultured in the presence of FGF-2 in solution differentiated into mesoderm tissue as indicated by Xbra expression. Animal caps that were cultured in the absence of FGF-2 in solution did not differentiate into mesoderm indicated by the absence of Xbra expression. These results indicate that in the presence of FGF-2 animal caps will differentiate into mesoderm and express the mesoderm gene marker Xbra. Animal caps induced with liquid-phase FGF-2 showed a dose response in Xbra expression. This expression seemed to plateau between 10ng/ml and 100ng/ml of FGF-2 in solution.

II. Solid-phase chamber design:

The solid-phase chamber consisted of four components: 1) Nitrocellulose paper, 2) stainless steel grid, 3) solid-phase glass slide, and 4) stack of washers for weight. Each one of these components went through rigorous testing to determine the requirements for each component. For the nitrocellulose, animal caps attached to NYTRAN paper the best out of the tested papers. Animal caps usually heal into balls, but adhesion to the NYTRAN paper allowed the animal caps to remain unhealed for more than 45min. This lack of healing was critical to allow the sensitive inner cells of the animal cap to be exposed to the solid-phase growth factors.

The second component, the stainless steel grid, was necessary for the precise placement of the animal caps and for isolation of each animal cap from one another.

The grid had to be thick enough to allow for the contact of the glass slide with the animal caps, while stopping the weight of the washers from crushing them. The final dimensions of the grid were 100um thick and a pore size of 700um across.

The glass slide was coated with fibrin as described in Material and Methods to allow for the adhesion of FGF-2. Miller et al. (2006) showed that there is little to no release of growth factor into the surrounding media after incubation of the fibrin coated glass slides containing FGF-2 for 24 hr in PBS. Once the slides have been blotted with FGF-2 and incubated in PBS for 24 hours, little or no FGF-2 was released into the surrounding media after 150 hours of being seeded with human MG-63 cells (Miller 2006). These results indicate that there was no soluble FGF-2, which would allow for liquid-phase exposure of the FGF-2.

The final component of the solid-phase chamber was five steel washers of one and a half inches in diameter. This weight was sufficient to maintain the contact between the glass slide and the animal caps.

III. Solid-phase induction with FGF-2:

a. RT-qPCR of solid-phase FGF-2 induced animal caps:

In the first RT-qPCR experiment, the animal caps showed a dose response in Xbra expression to the different concentrations of solid-phase FGF-2 presented. This is the first reported response of animal caps to the presentation of solid-phase FGF-2. In both controls, animal caps cultured in 20% Steinberg's and animal caps cultured in the solid-phase chamber in the absence of FGF-2, there was little or no expression of

Xbra. This result indicates that the response was due to the presence of solid-phase FGF-2 and not to the induced stress of being contained in the solid-phase chamber.

The experiment was repeated two more times. Both showed a dose response in Xbra expression to solid-phase FGF-2, as well as little or no expression of Xbra in either of the controls. Although the amount of Xbra expression varied in each experiment, I conclude that animal caps presented with solid-phase FGF-2 are induced to differentiate into mesoderm in a dose dependent manor, as shown by Xbra expression.

b. *In situ* examination of animal caps induced with solid-phase FGF-2:

In situ hybridization was performed with Xbra sense and antisense probes to assess further the response of animal caps to solid-phase FGF-2. The *in situ* was also performed to visualize any possible spatial patterns of the response. Animal caps were subjected to either induction via solid-phase FGF-2, or simply cultured in the solid-phase chamber in the absence of FGF-2. This second experiment was performed as a control to see if there was any response induced by the solid-phase chamber itself.

Animal caps that were induced with solid-phase FGF-2 and exposed to the antisense Xbra probe showed vivid staining in comparison to untreated animal caps subjected to the same staining. These results indicate that the animal caps that were induced with the solid-phase FGF-2 were responding with the expression of Xbra. In both, the treated and untreated animal caps exposed to the sense Xbra probe, there was no response indicated by the lack of staining.

This experiment was repeated giving the same results, although the levels of Xbra expression detected were lower. The difference in the amount of staining in the two experiments could be due to a couple of factors: 1) the time allowed for staining was 30 min less in the second experiment, 2) the animal caps were isolated from embryos of different frogs, or 3) the antisense probe used in each experiment was independently synthesized. In conclusion, the results of the in situ experiments support the RT-qPCR results that animal caps presented with solid-phase FGF-2 express Xbra, indicative of mesoderm induction.

IV. New solid-phase chamber design:

To more efficiently use this novel method a new solid-phase chamber had to be designed using the acquired knowledge from the previous experiments. The dimensions of the previously used grid have remained the same in the construction of the new grid. The grid insert contains 16 pores for animal cap placement, as well as grooves cut on the underside to allow for constant transport of oxygen and other necessary nutrients to the isolated animal caps (Fig. 9A). The chamber will utilize two screws for correct placement of the solid-phase growth factor containing glass slide. These screws will also apply the correct weight necessary for constant contact between the glass slide and the animal caps (Fig. 9B). The overall design will allow for printed patterns of growth factors to remain in registrar with the animal caps.

V. Future experiments with solid-phase growth factor presentation:

This novel approach to growth factor delivery can be applied to directly answer many development questions. There are three questions dealing with neural induction that can be specifically answered: (1) the mode of neural induction, (2) the formation of boundary tissues during neural induction, and (3) differential neural differentiation in response to concentration gradients. The first experiment that can be performed with this growth factor delivery approach is to determine the mode of neural induction. In simple terms, neural induction takes place when the organizer tissue migrates during gastrulation, ventrally underneath the overlying ectoderm. The two possible modes of induction are through the vertical release of the inhibitor molecules inducing neural tissue as it passes underneath the ectoderm, or a horizontal mode of induction with a single, initial release of inhibitor molecules at the dorsal lip (Fig. 10A)(Gamse and Sive, 2000). With solid-phase presentation, this experiment can be set up with animal caps, exposed to a simple pattern of noggin or another inhibitor molecule (Fig. 10B). An *in situ* hybridization could then be performed with a neural marker to show the mode of inhibition. If the natural induction process takes place via the vertical mode then you should only see a staining of the animal cap where the pattern of noggin was in direct contact with the cap (Fig. 10C). While on the other hand if the natural mode of induction is the horizontal one, then you should see a diffuse staining through out the animal cap or at least in an area larger than the pattern of noggin (Fig. 10C)

During this same time boundary tissues are being formed between tissues that are expressing BMP and where BMP is being inhibited (Wardle and Sive, 2003). This

question regarding boundary tissue formation has been looked at by manipulating the concentration of BMP and or the organizer molecules. Also, experiments reporting cement gland specific gene expression between neural and epidermal tissue lead to the hypothesis of boundary tissue formation (Wardle and Sive, 2003). Although these experiments have lead to a proposed hypothesis on boundary tissue formation, no definitive experiment has been done to show this. Using the solid-phase approach, an experiment could be set up by printing a pattern where one half of the glass slide will be coated with noggin and the other half will be coated with BMP. *In situ* hybridization could then be performed to see if the boundary tissue has formed between noggin and BMP induction.

Finally it has been proposed that during neural induction a concentration gradient is set up in the ectoderm by a gradient inhibition of BMP (Dale and Wardle, 1999). This inhibition is set up by the organizer releasing noggin along with other BMP binding proteins. This gradient is hypothesized to be responsible for the dorsoventral patterning of the neural tissue (Dale and Wardle, 1999). This question can be assayed with the solid-phase approach by printing a gradient pattern of noggin and exposing animal caps to this gradient. *In situ* hybridization with different gene specific probes will give a visual representation of the response to this proposed gradient hypothesis.

Conclusion

This novel approach to growth factor presentation has a similar effect on differentiation as the current liquid-phase approach, providing developmental biologists with an additional technique to test the effects of growth factors during development. This new approach will allow testing of patterns and multiple concentrations as well as multiple growth factors together. This also mimics in vivo induction more accurately because during development cells are being presented these growth factors directly from surrounding cells or bound to the extracellular matrix.

References

- Bernfield, M., Gotte, M., Park, P. W., Reizes, O., Fitzgerald, M. L., Lincecum, J. and Zako, M.** (1999). Functions of cell surface heparan sulfate proteoglycans. *Annu Rev Biochem* **68**, 729-77.
- Bijlsma, M. F., Spek, C. A. and Peppelenbosch, M. P.** (2004). Hedgehog: an unusual signal transducer. *Bioessays* **26**, 387-94.
- Biosystems Applied 2001 Use Bulletin #2** ABI Prism 7700 Sequence Detection System Applied Biosystems, CA.
- Bottcher, R. T. and Niehrs, C.** (2005). Fibroblast growth factor signaling during early vertebrate development. *Endocr Rev* **26**, 63-77.
- Campbell, P. G. and Andress, D. L.** (1997). Insulin-like growth factor (IGF)-binding protein-5-(201-218) region regulates hydroxyapatite and IGF-I binding. *Am J Physiol* **273**, E1005-13.
- Campbell, P. G. and Andress, D. L.** (1997). Plasmin degradation of insulin-like growth factor-binding protein-5 (IGFBP-5): regulation by IGFBP-5-(201-218). *Am J Physiol* **273**, E996-1004.
- Campbell, P. G., Durham, S. K., Hayes, J. D., Suwanichkul, A. and Powell, D. R.** (1999). Insulin-like growth factor-binding protein-3 binds fibrinogen and fibrin. *J Biol Chem* **274**, 30215-21.
- Campbell, P. G., Miller, E. D., Fisher, G. W., Walker, L. M. and Weiss, L. E.** (2005). Engineered spatial patterns of FGF-2 immobilized on fibrin direct cell organization. *Biomaterials* **26**, 6762-70.
- Campbell, P. G., Wines, K., Yanosick, T. B. and Novak, J. F.** (1994). Binding and activation of plasminogen on the surface of osteosarcoma cells. *J Cell Physiol* **159**, 1-10.
- Cornell, R. A. and Kimelman, D.** (1994). Activin-mediated mesoderm induction requires FGF. *Development* **120**, 453-62.
- Dailey, L., Ambrosetti, D., Mansukhani, A. and Basilico, C.** (2005). Mechanisms underlying differential responses to FGF signaling. *Cytokine Growth Factor Rev* **16**, 233-47.
- Dale, L. and Wardle, F. C.** (1999). A gradient of BMP activity specifies dorsal-ventral fates in early *Xenopus* embryos. *Semin Cell Dev Biol* **10**, 319-26.
- Delaune, E., Lemaire, P. and Kodjabachian, L.** (2005). Neural induction in *Xenopus* requires early FGF signalling in addition to BMP inhibition. *Development* **132**, 299-310.

- Durham, S. K., Suwanichkul, A., Hayes, J. D., Herington, A. C., Powell, D. R. and Campbell, P. G.** (1999). The heparin binding domain of insulin-like growth factor binding protein (IGFBP)-3 increases susceptibility of IGFBP-3 to proteolysis. *Horm Metab Res* **31**, 216-25.
- Eimon, P. M. and Harland, R. M.** (2002). Effects of heterodimerization and proteolytic processing on Derriere and Nodal activity: implications for mesoderm induction in *Xenopus*. *Development* **129**, 3089-103.
- Eisenberg, L. M. and Eisenberg, C. A.** (2006). Wnt signal transduction and the formation of the myocardium. *Dev Biol*.
- Fambrough, D., McClure, K., Kazlauskas, A. and Lander, E. S.** (1999). Diverse signaling pathways activated by growth factor receptors induce broadly overlapping, rather than independent, sets of genes. *Cell* **97**, 727-41.
- Fan, H., Liu, Y., Zhou, H., Wang, L., Li, W., Guo, L. and Roeske, R. W.** (2000). Selection of peptide ligands that bind to acid fibroblast growth factor. *IUBMB Life* **49**, 545-8.
- Gamse, J. and Sive, H.** (2000). Vertebrate anteroposterior patterning: the *Xenopus* neurectoderm as a paradigm. *Bioessays* **22**, 976-86.
- Gilbert, S. F.** (2000). *Developmental Biology*. Sunderland, MA: Sinauer Associates, Inc.
- Gurdon, J. B. and Bourillot, P. Y.** (2001). Morphogen gradient interpretation. *Nature* **413**, 797-803.
- Hemmati-Brivanlou, A., Kelly, O. G. and Melton, D. A.** (1994). Follistatin, an antagonist of activin, is expressed in the Spemann organizer and displays direct neuralizing activity. *Cell* **77**, 283-95.
- Hemmati-Brivanlou, A. and Melton, D.** (1997). Vertebrate embryonic cells will become nerve cells unless told otherwise. *Cell* **88**, 13-7.
- Isaacs, H. V., Pownall, M. E. and Slack, J. M.** (1994). eFGF regulates Xbra expression during *Xenopus* gastrulation. *Embo J* **13**, 4469-81.
- Kofron, M., Demel, T., Xanthos, J., Lohr, J., Sun, B., Sive, H., Osada, S., Wright, C., Wylie, C. and Heasman, J.** (1999). Mesoderm induction in *Xenopus* is a zygotic event regulated by maternal VegT via TGFbeta growth factors. *Development* **126**, 5759-70.
- Loose, M. and Patient, R.** (2004). A genetic regulatory network for *Xenopus* mesendoderm formation. *Dev Biol* **271**, 467-78.
- Martin, G. R.** (1998). The roles of FGFs in the early development of vertebrate limbs. *Genes Dev* **12**, 1571-86.

- Maurus, D. and Kuhl, M.** (2004). Getting an embryo into shape. *Bioessays* **26**, 1272-5.
- Miller, E. D., Fisher, G. W., Weiss, L. E., Walker, L. M. and Campbell, P. G.** (2006). Dose-dependent cell growth in response to concentration modulated patterns of FGF-2 printed on fibrin. *Biomaterials* **27**, 2213-21.
- Mohammadi, M., Schlessinger, J. and Hubbard, S. R.** (1996). Structure of the FGF receptor tyrosine kinase domain reveals a novel autoinhibitory mechanism. *Cell* **86**, 577-87.
- Nieuwkoop, P. D., and Faber.** (1956). Normal table of *Xenopus laevis*. *Daudin*.
- Nishida, H.** (2002). Patterning the marginal zone of early ascidian embryos: localized maternal mRNA and inductive interactions. *Bioessays* **24**, 613-24.
- Ohkawara, B., Iemura, S., ten Dijke, P. and Ueno, N.** (2002). Action range of BMP is defined by its N-terminal basic amino acid core. *Curr Biol* **12**, 205-9.
- Piccolo, S., Sasai, Y., Lu, B. and De Robertis, E. M.** (1996). Dorsoventral patterning in *Xenopus*: inhibition of ventral signals by direct binding of chordin to BMP-4. *Cell* **86**, 589-98.
- Ramos, J. W. and DeSimone, D. W.** (1996). *Xenopus* embryonic cell adhesion to fibronectin: position-specific activation of RGD/synergy site-dependent migratory behavior at gastrulation. *J Cell Biol* **134**, 227-40.
- Rifkin, D. B., Mazziere, R., Munger, J. S., Noguera, I. and Sung, J.** (1999). Proteolytic control of growth factor availability. *Apmis* **107**, 80-5.
- Ruhrberg, C., Gerhardt, H., Golding, M., Watson, R., Ioannidou, S., Fujisawa, H., Betsholtz, C. and Shima, D. T.** (2002). Spatially restricted patterning cues provided by heparin-binding VEGF-A control blood vessel branching morphogenesis. *Genes Dev* **16**, 2684-98.
- Sakiyama-Elbert, S. E. and Hubbell, J. A.** (2000). Development of fibrin derivatives for controlled release of heparin-binding growth factors. *J Control Release* **65**, 389-402.
- Sakiyama-Elbert, S. E. and Hubbell, J. A.** (2000). Controlled release of nerve growth factor from a heparin-containing fibrin-based cell ingrowth matrix. *J Control Release* **69**, 149-58.
- Sasai, Y., Lu, B., Steinbeisser, H. and De Robertis, E. M.** (1995). Regulation of neural induction by the Chd and Bmp-4 antagonistic patterning signals in *Xenopus*. *Nature* **376**, 333-6.
- Schier, A. F. and Shen, M. M.** (2000). Nodal signalling in vertebrate development. *Nature* **403**, 385-9.

- Schulte-Merker, S. and Smith, J. C.** (1995). Mesoderm formation in response to Brachyury requires FGF signalling. *Curr Biol* **5**, 62-7.
- Shi, Y. and Massague, J.** (2003). Mechanisms of TGF-beta signaling from cell membrane to the nucleus. *Cell* **113**, 685-700.
- Shook, D. R., Majer, C. and Keller, R.** (2004). Pattern and morphogenesis of presumptive superficial mesoderm in two closely related species, *Xenopus laevis* and *Xenopus tropicalis*. *Dev Biol* **270**, 163-85.
- Slack, J. M.** (1991). The nature of the mesoderm-inducing signal in *Xenopus*: a transfilter induction study. *Development* **113**, 661-9.
- Slack, J. M., Darlington, B. G., Heath, J. K. and Godsave, S. F.** (1987). Mesoderm induction in early *Xenopus* embryos by heparin-binding growth factors. *Nature* **326**, 197-20
- Smith, J. C.** (1989). Mesoderm induction and mesoderm-inducing factors in early amphibian development. *Development* **105**, 665-77.
- Smith, J. C.** (1989). Mesoderm induction and mesoderm-inducing factors in early amphibian development. *Development* **105**, 665-77.
- Smith, W. C., Knecht, A. K., Wu, M. and Harland, R. M.** (1993). Secreted noggin protein mimics the Spemann organizer in dorsalizing *Xenopus* mesoderm. *Nature* **361**, 547-9.
- Smith, W. C., McKendry, R., Ribisi, S., Jr. and Harland, R. M.** (1995). A nodal-related gene defines a physical and functional domain within the Spemann organizer. *Cell* **82**, 37-46.
- Song, K., Takemaru, K. I. and Moon, R. T.** (1999). A role for xGCNF in midbrain-hindbrain patterning in *Xenopus laevis*. *Dev Biol* **213**, 170-9.
- Stern, C. D.** (2005). Neural induction: old problem, new findings, yet more questions. *Development* **132**, 2007-21.
- Strigini, M. and Cohen, S. M.** (2000). Wingless gradient formation in the *Drosophila* wing. *Curr Biol* **10**, 293-300.
- Sun, B. I., Bush, S. M., Collins-Racie, L. A., LaVallie, E. R., DiBlasio-Smith, E. A., Wolfman, N. M., McCoy, J. M. and Sive, H. L.** (1999). derriere: a TGF-beta family member required for posterior development in *Xenopus*. *Development* **126**, 1467-82.
- Thomsen, G. H. and Melton, D. A.** (1993). Processed Vg1 protein is an axial mesoderm inducer in *Xenopus*. *Cell* **74**, 433-41.

- Tucker, A. S. and Slack, J. M.** (2004). Independent induction and formation of the dorsal and ventral fins in *Xenopus laevis*. *Dev Dyn* **230**, 461-7.
- Valentino, L. and Pierre, J.** (2006). JAK/STAT signal transduction: regulators and implication in hematological malignancies. *Biochem Pharmacol* **71**, 713-21.
- van der Wees, J., Schilthuis, J. G., Koster, C. H., Diesveld-Schipper, H., Folkers, G. E., van der Saag, P. T., Dawson, M. I., Shudo, K., van der Burg, B. and Durston, A. J.** (1998). Inhibition of retinoic acid receptor-mediated signalling alters positional identity in the developing hindbrain. *Development* **125**, 545-56.
- Wardle, F. C. and Sive, H. L.** (2003). What's your position? the *Xenopus* cement gland as a paradigm of regional specification. *Bioessays* **25**, 717-26.
- Wardle, F. C. and Smith, J. C.** (2004). Refinement of gene expression patterns in the early *Xenopus* embryo. *Development* **131**, 4687-96.
- Yasuo, H. and Lemaire, P.** (1999). A two-step model for the fate determination of presumptive endodermal blastomeres in *Xenopus* embryos. *Curr Biol* **9**, 869-79.
- Yokoyama, H., Ide, H. and Tamura, K.** (2001). FGF-10 stimulates limb regeneration ability in *Xenopus laevis*. *Dev Biol* **233**, 72-9.
- Zhang, J., Houston, D. W., King, M. L., Payne, C., Wylie, C. and Heasman, J.** (1998). The role of maternal VegT in establishing the primary germ layers in *Xenopus* embryos. *Cell* **94**, 515-24.